Volume 62
Number 28
14 April 2026
Pages 7209–7432

ChemComm

Chemical Communications

rsc.li/chemcomm

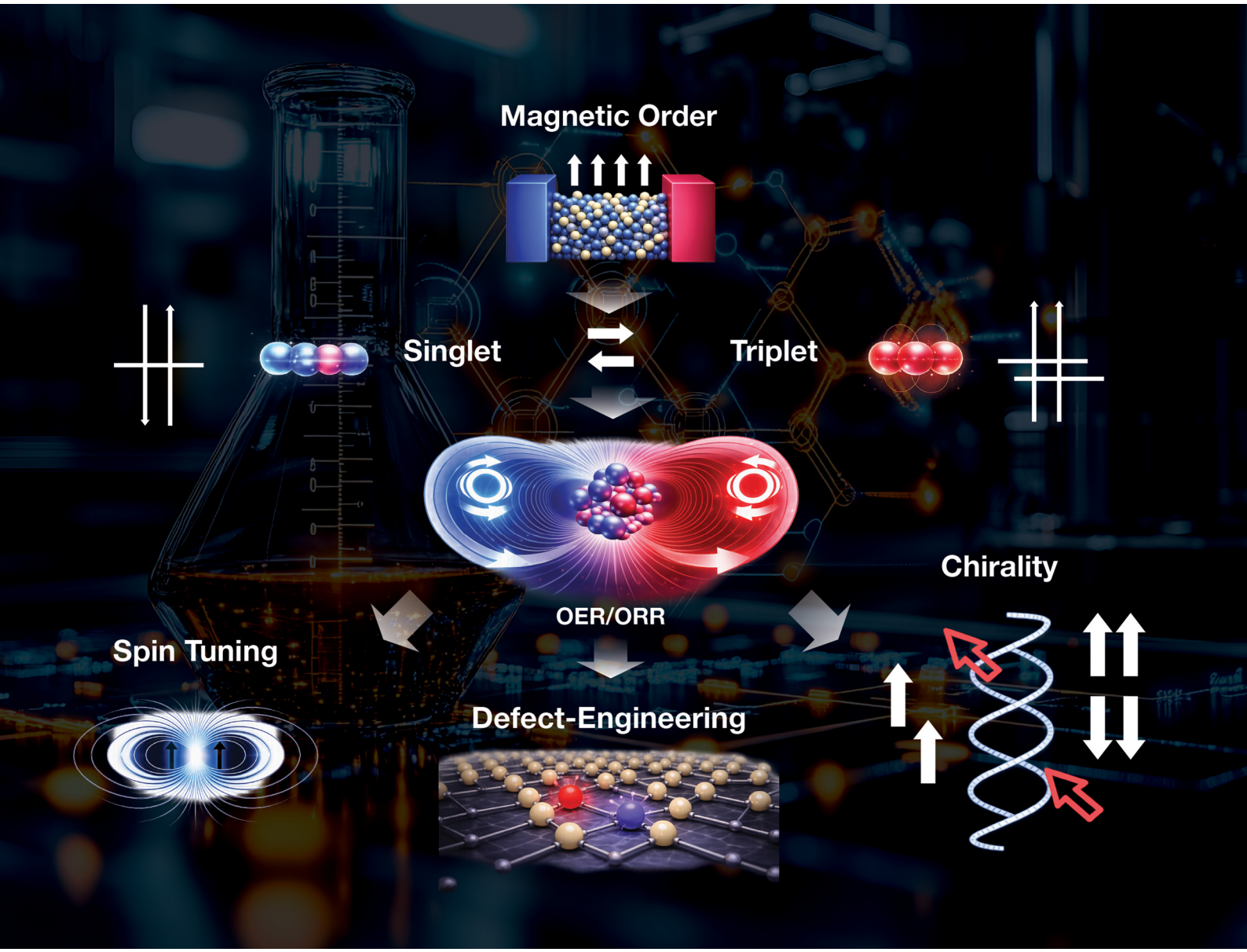

ISSN 1359-7345

ROYAL SOCIETY OF CHEMISTRY

REVIEW ARTICLE

Kenneth I. Ozoemena *et al.*

Construction, computation, and characterisation of spin-control powered catalysts for oxygen electrocatalysis

ChemComm

REVIEW ARTICLE

View Article Online
View Journal | View Issue

Cite this: *Chem. Commun.*, 2026, **62**, 7248

Construction, computation, and characterisation of spin-control powered catalysts for oxygen electrocatalysis

Ernst H. Hechter, [a] Augustus K. Lebechi, [a] Desalegn N. Gemechu, [ab] Fitsum A. Hailu, [a] Dean H. Barrett, [a] Lesego Gaolathe, [a] Thapelo P. Mofokeng [a] and Kenneth I. Ozoemena [*a]

Spin has emerged as a powerful and complementary dimension in the rational design of oxygen electrocatalysts, offering a route to circumvent long-standing limitations imposed by conventional activity descriptors and scaling relationships. This review consolidates recent advances demonstrating how spin states, magnetic ordering, and spin-selective electron transport influence the thermodynamics and kinetics of key OER and ORR steps, particularly the spin-forbidden transition from singlet intermediates to triplet oxygen. We critically examine traditional strategies such as ligand-field engineering, doping, lattice strain, and defect control, as well as spin polarisation approaches including magnetic-field assistance and chiral-induced spin selectivity (CISS), integrating insights from theory, computation, and *operando* characterisation. Collectively, these studies reveal that manipulating spin polarisation at active sites can accelerate multi-electron transfer pathways, alter intermediate binding, and enhance overall catalytic performance beyond classical design limits. Finally, we highlight remaining mechanistic ambiguities, emerging diagnostic tools, and future opportunities for integrating spin physics into scalable electrocatalyst development.

Received 19th December 2025,
Accepted 10th February 2026

DOI: 10.1039/d5cc07243c

rsc.li/chemcomm

[a] *Molecular Science Institute, School of Chemistry, University of the Witwatersrand, Johannesburg 2050, South Africa. E-mail: kenneth.ozoemena@wits.ac.za*
[b] *Department of Chemistry, College of Natural and Computational Sciences, Addis Ababa University, Addis Ababa 1176, Ethiopia*

Introduction

Oxygen reduction and evolution

The need for new energy generation, storage and conversion technologies has become clear. On the one hand, archaic methods of burning fossil fuel generate airborne carbon,

Ernst H. Hechter

Ernst H. Hechter obtained his MSc degree while researching magnetic enhancement in electrocatalysis at the School of Chemistry at the University of the Witwatersrand in 2023. He is currently pursuing his PhD under supervision of Dr Dean Barrett and Professor Kenneth Ozoemena in the DSI-NRF-Wits SARChI Chair in Materials for Energy and Electrochemistry Technologies (MEET) group, investigating the chiral spin selection effect in metal–air battery systems. His research interests lie in electrocatalysis and materials characterisation for sustainable development.

Augustus K. Lebechi

Dr Augustus K. Lebechi is Postdoctoral Research Fellow in the DSI-NRF-Wits SARChI Chair in Materials Electrochemistry and Materials Technologies (MEET) at the School of Chemistry of the University of the Witwatersrand (Wits). He holds a PhD in Chemistry from Wits (2023) under the supervision of Prof. KI Ozoemena. His research interests are in materials science, electrocatalysis, green hydrogen production and batteries.

sulphur, and nitrogen species with adverse effects on local environments and human health, not to mention global impacts such as radiative forcing and ocean acidification. On the other hand, growing energy demand and rapidly proliferating energy-hungry technologies such as artificial intelligence require that energy be available for mobile or isolated systems. Oxygen evolution reaction (OER) and oxygen reduction reaction (ORR) electrocatalysis have a critical role in powering the transition to ecologically clean energy, with applications in water splitting, fuel cells and metal–air batteries.[1] OER is a bottleneck process occurring at the anode side of the water electrolysis: its sluggish kinetics drags down the overall reaction rate and energy efficiency of the system. ORR, the reverse reaction, appears at the cathode of fuel cells and, in metal–air batteries, converts oxygen gas into water *via* a redox process. The onset potential of ORR limits the voltage that such devices may supply.[2,3] Enhancing and optimizing these oxygen-involved electrocatalysis processes through catalyst design is vital for developing electrochemical devices with better energy conversion efficiency and total performance. Works to develop effective catalysts have continued toward accelerating the kinetics of OER and ORR, employing various material design strategies that rely on growing the density as well as the intrinsic activity of active sites, for example p- and d-band centre, d-electron number, e_g orbital filling, charge-transfer energy, and p–d hybridization, among others.[4–6]

While these structural and electronic descriptors have successfully guided catalyst optimisation for decades, they describe only the energetic landscape of adsorption and bond formation-not the fundamental quantum constraints governing how electrons move during the reaction. Oxygen-involving electrocatalysis is intrinsically spin-dependent: intermediates such as *OH and *O exist as singlets, whereas O_2 has a triplet ground state, and interconversion between these states is formally spin-forbidden.[8] Conventional catalyst design therefore overlooks an essential degree of freedom-electron spin-which directly influences reaction kinetics through spin selection rules and exchange interactions as well as associated

Desalegn N. Gemechu

Desalegn N. Gemechu is a computational chemist with expertise in first-principles simulations, particularly using DFT to study energy storage and conversion systems. In 2024, Dr Gemechu was an ESIMSAD-Visiting Scholar in the DSI-NRF-Wits SARChI Chair in Materials Electrochemistry and Materials Technologies (MEET) at the School of Chemistry of the University of the Witwatersrand.

Fitsum A. Hailu

Fitsum Addis Hailu is a final year PhD candidate (in water-splitting and metal–air batteries) under the supervision of Prof Ozoemena at the University of the Witwatersrand South Africa. He holds a degree in Mechanical Engineering and MSc in Materials Science. He is a Lecturer at the Addis Ababa University where he teaches materials science and engineering.

Dean H. Barrett

Dr Dean H. Barrett is a Senior Lecturer and Researcher in Physical Chemistry at the University of the Witwatersrand (Wits). He holds a PhD in Physical-Inorganic Chemistry from Wits (2012). His research is focused on the development and characterisation of materials (catalysts, energy, biomass, and functional materials). He also works as a beamline scientist, developing new instrumentation and experimental designs required to study modern materials at synchrotron facilities. He serves as a joint appointment researcher (Heterogeneous and hierarchical matter division) at the LNLS (Brazil).

Lesego Gaolathe

Dr Lesego Gaolatlhe is Postdoctoral Research Fellow in the DSI-NRF-Wits SARChI Chair in Materials Electrochemistry and Materials Technologies (MEET) at the School of Chemistry of the University of the Witwatersrand (Wits). She holds a PhD in Chemistry from Wits (2024) under the supervision of Prof KI Ozoemena. Her research focus is focussed on rational synthesis of electrode materials for electrocatalysis and development of rechargeable zinc–based batteries.

thermodynamic effects such as changes in magnetic entropy.[9] Recognising spin as a catalytic descriptor opens an orthogonal design space in which active-site spin state, magnetic ordering, external fields, and chiral environments can be engineered to accelerate steps historically limited by slow spin transitions. In the following sections, we explore how spin control has emerged as a powerful and versatile tool for breaking long-standing activity constraints in both OER and ORR.[4,10]

Increasing effort has been made to develop spin-selective catalysts to take advantage of these effects.[11] Although various reviews in this area have been published recently, few categorize and evaluate spin-selective catalysts according to the source of spin polarisation. Therefore, recognizing the most advanced spin-selective catalysis of OER and ORR is beneficial and crucial.

The development of spin-selective catalysts requires the presence of spin-polarized adsorption sites, which can be demonstrated by primarily describing the basic principles of spin-selectivity using the spin-sensitive reaction pathways of OER and ORR.[8,10,12] Afterwards, approaches for examining the spin-related transition during electrocatalysis through theoretical calculations and *in situ* and *operando* characterisation methods. The unresolved concerns and future possibilities in this area can finally be addressed with the goal of providing a clear path for developing innovative and extremely effective spin-polarized electrocatalysis that involves industrial oxygen evolution and reduction reaction processes.

Spin physics in brief

The term ''electron spin'' will be familiar to anyone who has undergone undergraduate training in the natural sciences. The term is somewhat misleading as electrons are not classical objects that may rotate, despite this analogy's popularity in chemistry education. Rather, spin is a symmetry property of quantum particles. Electrons belong to the family of particles called leptons which are themselves in the class of the fermions, which are particles with half integer spins. These particles, which include quarks, make up all matter.[13] While spin may seem on the surface to be somewhat esoteric, it is in fact the property that allows matter to exist as discrete atoms at all *via* the Pauli exclusion principle: fermions with identical quantum numbers cannot spatially overlap. This fundamental property of nature is what gives rise to chemistry: electrons cannot have identical wavefunctions despite being bound to the same atomic nucleus, and so they segregate into the ''atomic orbitals'' each capable of accommodating two electrons of identical angular momentum but opposite in spin: one has spin +1/2 and is called spin-up, and the other is spin down with a spin of −1/2.[14]

Here nature shows a curious agreement with the ''rotating ball'' analogy. Electrons have another intrinsic quantum property generally called negative electric charge and, through interaction with their spin, they have a magnetic moment. The direction of the magnetic moment depends on the sign of the electron's spin, almost as if the electron really were a spinning little charged sphere.

Conversion between spin states is quantum-mechanically forbidden: most transitions require that the initial and final states have the same spin, a phenomenon similar to conservation of angular momentum. This would put a damper on our dreams of OER and ORR, as the parallel electrons of triplet oxygen can never pair up to allow conversion to singlet water, or vice versa. (It is worth noting that this obstacle is all that stands in the way of the incineration of earth's surface by atmospheric oxygen).[15]

However, one must also consider the magnetic field produced by the orbital angular momentum of the electron about its nucleus. The interaction between the magnetic fields from the electron's spin angular momentum and its orbital angular momentum is known as spin–orbit coupling. An electron with its spin such that its orbit and spin are parallel is in a lower energy state than one with these vectors antiparallel, contributing to the fine structure seen in spectroscopy experiments. The

Thapelo P. Mofokeng

Dr Thapelo P. Mofokeng is a Research Associate in the DSI-NRF-Wits SARChI Chair in Materials Electrochemistry and Materials Technologies (MEET) and Lecturer at the School of Chemistry of the University of the Witwatersrand (Wits). He holds a PhD in Chemistry from Wits (2021) under the supervision of Prof. KI Ozoemena and Dr Z Tetana. His research interest in focused on rational design of electrode materials for batteries, supercapacitors, and energy-related conversion technologies.

Kenneth I. Ozoemena

Kenneth I. Ozoemena is a Research Professor at the University of the Witwatersrand where he heads the South African DSI-NRF-Wits SARChI Chair (Tier 1) in Materials Electrochemistry and Materials Technologies (MEET). Ken holds a PhD in Chemistry from Rhodes University (2003). His research focus is on energy storage and conversion. He is South Africa's A-rated Scientist and recipient of the prestigious gold medal of the South African Chemical Institute (SACI). He is Editor-in-Chief of Electrochemistry Communications and serves on the editorial board of ChemComm. Prof Ozoemena is an Adjunct Professor at the Department of Mechanical Engineering and Engineering Science of the University of North Carolina at Charlotte, USA.

other contributions to fine structure are the couplings between the spin and orbital momenta and the magnetic moment of the nucleus itself. The energy difference between electron states with parallel and antiparallel spins is:

$$\Delta E = \frac{\lambda}{2}(j(j+1) - l(l+1) - s(s+1))$$

The interaction is more significant for heavier elements, becoming more significant with increasing atomic number Z.[16] The spin orbit coupling constant λ can be expressed as:

$$\lambda_{n,l} = Z^4 \frac{\mu_0}{4\pi} {g_s}{\mu_B}^2 \frac{1}{n^3 \alpha^3 l\left(l+\frac{1}{2}\right)(l+1)}$$

where Z is the atomic number, μ_0 is the permeability of free space, g_s is the electron spin g factor, μ_B is the Bohr magneton, n is the principal quantum number of the electron, l is the orbital angular momentum quantum number and α is the fine structure constant

This coupling "mixes" wavefunctions and so opens the possibility for electrons to change their spin, a process called intersystem crossing. Part of the reason why heavy precious metal catalysts are so effective for the oxygen reactions is that they facilitate spin-state changes through spin–orbit coupling.[17] In this review we explore how intersystem crossing may be enhanced even in systems of lighter atoms, through electron orbital energy tuning, geometric influences, and long range magnetic interactions.

Electron spin also has consequences for the flow of electric charge. Electrons moving through the conduction band of a material must occupy vacant orbitals, where they experience spin–orbit coupling. The interaction between the external electric field and the coupling causes electrons with opposite spins to be deflected in perpendicular directions, leading to buildups of parallel spin on opposite sides of the conducting material, which can be measured experimentally. This accumulation of parallel spin electrons is referred to as spin polarisation or magnetic ordering, as these electrons' intrinsic magnetic fields reinforce one another to create a local magnetic field. An alternative explanation is the Mott scattering mechanism, where a classical (rotating ball) electron travels towards a positively charged atomic nucleus. Due to the nucleus's motion relative to the electron, a magnetic field is experienced by the electron. This will necessarily deflect electrons of opposite spin in opposite directions. Both mechanisms are interesting in that they allow the segregation of electrons with different spin states, allowing the conception of spin-filtering devices. Indeed, such devices may prove valuable in next-generation spintronic computing. Our interest here, however, is in the little explored use of such filters in chemistry, in both application and computation.

Spin-selective oxygen electrocatalysis

Mechanisms

The four-electron reaction process, which has been used to explain the catalytic mechanism of many material systems, can be used to characterize the reaction pathways of OER (eqn (1) to (4) and (5) to (8)) and ORR (eqn (4) to (1) and (8) to (5)). The adsorption sites are indicated by the symbol "*", and the arrows "↑" and "↓" indicate the spin direction of HOMO electrons.[18,19] In acidic media:

$$H_2O(\uparrow\downarrow) + * \rightarrow *OH(\uparrow) + H^+ + e^-(\downarrow) \quad (1)$$

$$*OH(\uparrow) \rightarrow *O(\uparrow\downarrow) + H^+ + e^-(\uparrow) \quad (2)$$

$$*O(\uparrow\downarrow) + H_2O(\uparrow\downarrow) \rightarrow *OOH(\uparrow\downarrow\uparrow) + H^+ + e^-(\downarrow) \quad (3)$$

$$*OOH(\uparrow\downarrow\uparrow) \rightarrow * + O_2(\uparrow\uparrow) + H^+ + e^-(\downarrow) \quad (4)$$

And in basic media:

$$OH^-(\uparrow\downarrow\uparrow\downarrow) + * \rightarrow *OH(\uparrow\downarrow\uparrow) + e^-(\downarrow) \quad (5)$$

$$*OH(\uparrow\downarrow\uparrow) + OH^-(\uparrow\downarrow\uparrow\downarrow) \rightarrow *O(\uparrow\downarrow\uparrow\downarrow) + H_2O(\uparrow\downarrow) + e^-(\uparrow) \quad (6)$$

$$*O(\uparrow\downarrow\uparrow\downarrow) + OH^-(\uparrow\downarrow\uparrow\downarrow) \rightarrow *OOH(\uparrow\uparrow\downarrow) + e^-(\downarrow) \quad (7)$$

$$*OOH(\uparrow\uparrow\downarrow) + OH^-(\uparrow\downarrow\uparrow\downarrow) \rightarrow * + O_2(\uparrow\uparrow) + H_2O(\uparrow\downarrow) + e^-(\downarrow) \quad (8)$$

Overall, three electrons with parallel spin and one with opposite spin must be transferred. The outer electrons of oxygen within reactant H_2O are paired with hydrogen, and H_2O as well as OH^- are spin-singlets. Through the removal of one spin-down electron from H_2O, the *OH is formed and adsorbed on the active sites of catalysts, in step 1. Afterward, the unpaired spin-up electron of *OH will be further removed to form *O in step 2. Therefore, it can be seen that the removal of electrons with either spin-up or spin-down orientation in step 1 does not affect the electron spin configuration of the products (*i.e.*, *O) in step 2. The spin-sensitive electron transfer is attributed to the O–O coupling in steps 3 and 4 because a spin-state transition is needed owing to the different spin-state of *O (spin-singlet) and O_2 (spin-triplet). Specifically, in the case of spin alignment, the spin direction of electrons transferred from *O in step 3 is parallel to the ones removed from *OOH, which benefits the formation of triplet oxygen. In contrast, if the two removal electrons in steps 3 and 4 are spin-unaligned, additional energy consumption will be needed to form the excited singlet dioxygen molecule. Thus materials with spin-selective functionality will be more efficient than other materials.[2,19] This reasoning holds whether the specific mechanism resembles the simple Adsorbate Evolution Mechanism (AEM) or the Lattice Oxygen Evolution Mechanism (LOM).[20]

Gracia *et al.* in 2017 identified magnetic entropy as another factor in the kinetics of these oxygen reactions. The effect may be non-rigorously explained as follows: reactions that result in a spin change must accept or donate electrons of parallel spin.

Table 1 Recent OER catalysts

OER				
Catalyst	Overpotential (mV@mA cm^{-2})	Electrolyte	Durability (h@mA cm^{-2})	Ref.
$Mn_{0.4}Ru_{0.6}O_2$	196@10	0.5 M H_2SO_4	120@10	22
Mn–RuO_2	143@10	0.5 M H_2SO_4	480@10	23
Ni1–MoS_2	437@100	1.0 M KOH	NA	24
CF-FeSO	192@10	1.0 M KOH	150@100	25
Ce-CoP	240@10	1.0 M KOH	25@10	26
$MgFeN_5C$	224@10	1.0 M KOH	15@10	27
Ni_3Fe-CW	266@10	1.0 M KOH	50@10	28
CrMnFeCoNi	315@10	1.0 M KOH	300@10	29
$CoFe_2O_4$	522@100	1.0 M KOH	20@10	30

Table 2 Recent ORR catalysts

ORR				
Catalyst	E_{onset} (V)/$E_{1/2}$ (V)	Electrolyte	Durability (h@mA cm^{-2})	Ref.
High-spin Fe(III)-N–C	1.0/0.86	0.1 M KOH	70@20	31
FeCoNi@NC	NA/0.918	0.1 M KOH	8@6.5	32
FeCo-MHs	1.05/0.95	0.1 M KOH	550@20	33
CoFe-NG	NA/0.95	0.1 M KOH	250@5	34
CoNi@NC	0.98/0.86	0.1 M KOH	18@NA	35

If they interact with a catalyst surface with equal populations of spin-up and spin-down electrons, this interaction will cause a spin imbalance and hence a decrease in entropy, making the process less thermodynamically favourable. In contrast, if the surface already has an excess of correctly oriented electrons, there is no change in entropy during the electron transfer.[9]

Most research in this field focuses on common materials with intrinsic ferromagnetism, such as Fe-, Co-, and Ni-based alloys and compounds. However, their intrinsic activity lags behind that of noble metal catalysts. Some recent oxygen catalysts are arranged in Tables 1 and 2

Therefore, to accelerate OER and ORR kinetics from the perspective of spin-selective electron transfer, the primary task is to develop spin-polarized materials with considerable conductivity and intrinsic activity.[21] Advances in computation and characterisation open the door to rational design of such materials.

Computation

Density functional theory (DFT) is a computational quantum mechanical method that allows us to study the electronic structure of materials and catalysts at the atomic level. In electrocatalysis, DFT provides detailed insights into how electrons are distributed in a catalyst, how molecules adsorb, and how chemical reactions proceed. By solving the quantum mechanical equations for electrons in a system, DFT predicts the total energy, spin states, and magnetic properties of catalysts and intermediates.[36]

One of the key advantages of DFT is its ability to capture spin polarisation in materials, which is essential for understanding

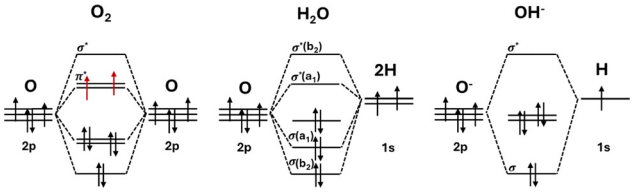

Fig. 1 Schematic orbital filling of reactants OH^-, H_2O and the triplet ground state O2 and their representative magnetic states. Redrawn with permission.[7] Copyright 2025, Wiley-VCH.

spin-dependent reactions in ORR and OER. DFT calculations can reveal which spin channels are favoured for electron transfer, how magnetic ordering in catalysts (ferromagnetic or antiferromagnetic) influences reactivity, and which reaction pathways are spin-allowed or spin-forbidden.

As illustrated in Fig. 1 from van der Minne *et al.*,[7] the oxygen evolution reaction (OER) often proceeds slowly and requires a high overpotential partly because the spin states of the reactants and product do not match. The reactants, such as hydroxide (OH^-) or water (H_2O) depending on the pH, have paired electrons and are therefore diamagnetic, while the product, molecular oxygen (O_2), has two unpaired electrons in its triplet ground state, making it paramagnetic. This difference means that the overall spin is not conserved during the reaction, so the process is considered spin-forbidden under the spin selection rule.

In their comprehensive study, Li *et al.*[4] employed DFT to systematically investigate how spin-selective catalysts can enhance the kinetics of oxygen-involved electrocatalytic reactions specifically the OER and ORR by promoting spin-polarized electron transfer, stabilizing spin-compatible reaction intermediates such as O_2, OOH, and OH, and modulating the magnetic interactions at active sites, thereby offering a novel, non-compositional strategy to improve catalytic performance through the deliberate control of spin alignment and magnetic ordering.[4]

DFT also allows us to explore the effects of magnetic materials, heterostructures, and spin–orbit interactions. For example, spin-polarized DFT can show how Fe, Co, Ni, or Mn centres in catalysts create spin-dependent adsorption sites for oxygen species, explaining why certain spin-active metals enhance ORR or OER activity. Including spin–orbit coupling in DFT further enables predictions of subtle spin effects, such as those observed in chiral-induced spin selectivity (CISS), which can influence reaction selectivity.

Additionally, DFT provides quantitative data such as adsorption energies, reaction barriers, density of states (DOS), and charge transfer, which can guide the design of new catalysts. By combining DFT results with experimental observations, researchers can identify the electronic and spin features that make a catalyst efficient, selective, and robust.

Overall, DFT is an indispensable tool for understanding the electronic and spin-level mechanisms of electrocatalysis and for rationally designing catalysts with optimized performance, supporting and being supported by advanced characterisation techniques.

Characterising spin-dependent pathways

The characterisation of spin polarised electrocatalysts for OER and ORR presents unique challenges that require a multiscale approach to fully elucidate the interplay between structural chirality, spin effects, and catalytic performance. Emerging and *operando* techniques represent the frontier of state-of-the-art characterisation, allowing real-time observation of dynamic processes. These methods integrate spectroscopy, diffraction and scattering, microscopy, and electrochemistry to capture transient chiral and spin changes during OER/ORR, bridging static structural data with operational performance.

Emphasis has been placed on *in situ*/*operando* insights into OER mechanisms across acidic/alkaline media, incorporating synchrotron techniques like X-ray Magnetic Circular Dichroism (XMCD) to probe magnetic/spin effects in chiral electrocatalysts. These methods are increasingly integrated with magnetic fields to amplify CISS signals, as noted in roadmaps for spin-enhanced OER.[37]

Recent years have seen noticeable progress in *operando* synchrotron methods applied to electrocatalysts, including those with chiral and spin-related features for OER/ORR. These advances focus on high spatial and temporal resolution probes that capture dynamic spin polarisation, structural chirality, and intermediate species under operating electrochemical conditions. For instance, high-energy resolution fluorescence-detected X-ray absorption spectroscopy (HERFD-XAS) has been highlighted for its ability to resolve fine electronic and spin state changes in OER catalysts, such as Mn and Cr-based oxides. This technique has been used to track *operando* changes in oxidation states and spin configurations, revealing how chiral environments reduce overpotentials by favouring triplet O_2 formation.[38]

Operando X-ray absorption spectroscopy (XAS), including X-ray absorption near-edge structure (XANES) and extended X-ray absorption fine structure (EXAFS) experiments, track changes in metal oxidation states and local geometry, while X-ray Emission Spectroscopy (XES) probes the electronic structure *via* fluorescence. Specifically, when applied to OER/ORR, these methods monitor shifts in metal d-orbitals, revealing spin state transitions (*e.g.*, low-to-high spin) that facilitate O–O coupling in OER.

Overall, synchrotron advances are shifting toward multimodal setups where multiple techniques are combined in unison for comprehensive structure-spin-activity correlations.

Numerous recent examples abound, such as the application of *operando* spectroscopy in chiral metal–organic frameworks (MOFs),[39] and *operando* electrochemical/spectroscopic evidence of CISS in chiral Fe–Ni oxides for OER.[40] A particularly relevant advancement is the use of *operando* electrochemical and spectroscopic tools to directly link chirality to enhanced OER kinetics, as demonstrated in studies on chiral-modified catalysts.[12] Here, synchrotron-based X-ray absorption near-edge structure (XANES) and extended X-ray absorption fine structure (EXAFS) under bias confirmed spin-polarised pathways in chiral systems, showing faster electron transfer and reduced peroxide intermediates in ORR. Similarly, *operando* XAS has revealed preferential structural evolution in non-noble metal heteroatom compounds for OER, where spin-dependent mechanisms were probed in real-time. For acidic OER on RuO_2, *operando* synchrotron methods identified oxide path mechanisms with varying oxygen species, potentially extendable to chiral variants to study spin filtering.[22]

Spin control in the mainstream

The main consideration of electron spin in catalysis has been the spin state of active metal ions' valence d orbitals. The five d orbitals have different orientations in space and so are split in energy when in a ligand field that is not perfectly spherically symmetrical. For example, in an octahedral field there are 6 ligands surrounding the metal at the vertices of an octahedron. Electrons in orbitals that point directly towards the ligands would create additional electromagnetic repulsion, and so the d_{z^2} and $d_{x^2-y^2}$ orbitals are raised in energy to form the doubly degenerate e_g orbitals, while the lower energy d_{xy}, d_{xz}, and d_{yz} form the triply degenerate t_{2g} orbitals. The gap in energy between the orbitals depends on the magnitude of the ligand field, essentially how strong the interaction between the ligands and the metal ion is. When this field is strong, electrons will fully populate the t_{2g} orbitals first: an ion with 5 d electrons, such as Mn^{2+}, will have an electron configuration with all 5 electrons in the t_{2g} orbitals: a low-spin configuration. Energy is required to pair electrons in an orbital, and unpaired electrons with parallel spins are stabilised in energy and have greater entropy. When these effects outweigh the field splitting, the state with 3 t_{2g} and 2 e_g electrons may be favoured. This is the high-spin state, so called because more electrons are unpaired and parallel. For our Mn^{2+} ion, this is the difference between a doublet in the low-spin state, and a sextet in the high-spin state.

The generally superior performance of intermediate to high-spin transition metal catalysts have historically been ascribed to optimised binding energy: empty e_g orbitals would accept donor electrons from reactants too readily, and the products would remain strongly chemisorbed to the catalyst surface, while partially filled orbitals could allow optimisation of the binding energy.[41] Hence, on that old staple of catalysis, the volcano plot, high-spin metal ions should be seen closer to the peak of the volcano. Spin control also has a deeper influence than well-tuned binding energies. Work on perovskites in the 2010's showed that the ordering of catalyst spins was vital in facilitating the spin changes needed for OER.[42–44] As is seen in radical chemistry, the alignment of electron spin states serves to avoid high energy intermediates such as singlet oxygen.[45,46] It should be noted that considerations of spin do not end at metal d orbitals: the filling of other atomic or molecular orbitals in composite catalysts have also been found to affect electrochemical performance.[47]

Several strategies have been formulated to control the spin state of a given system. Where ligands can be exchanged, weakening the ligand field is an obvious route to stabilise the high-spin state. This involves replacing strong field ligands,

where electron orbitals that overlap strongly with metal d orbitals, with weaker field ligands, including harder anions.[48] The degree of interaction between the ligand and metal may also be tuned by ''strain engineering'' where stress in the catalyst nanoparticle can force the ligand physically closer or further from the metal, increasing or decreasing the field splitting, respectively.[41] This approach can be expanded by including other metal species that may modify the field strength and electron density, through metal doping[49] or synthesis of heterostructures.[50]

Lattice straining

The adaptation of stress to the lattice structure and orientation of the electrocatalyst has an overwhelming impact on the coordination and structure of the metal centre, distorting the symmetry of the actual crystal lattice. When the lattice structure changes, the coordination environment around the metal site will also be modified, possibly leading to a change in its spin state. This shift can influence electrocatalytic activity and selectivity, as the spin state of the active site is associated with its electrocatalytic activity. Therefore, understanding catalyst crystallization and stress, including lattice orientation at the active centre, is vital for electrocatalyst design and optimization.[51]

A model system for tensile strain can be seen in the ultrathin nanosheets of a metal–organic framework (DD-Ni-NDA). The impact of tensile strain and unsaturated coordination flaws on overall spin state were explained by He *et al.*[52] The results obtained from zero-field cooling or ZFC temperature-dependent magnetic susceptibility showed that more unpaired electrons occupied the e_g orbital in pristine Ni-NDA; however, few unpaired electrons were present in the e_g orbital in DD-Ni-NDA nanosheets. Therefore, Ni^{2+} in pristine Ni-NDA is a high-spin state ($d_{z^2} = 1$) and Ni^{2+} in DD-Ni-NDA nanosheets is a low-spin state ($d_{z^2} = 0$). The transformation in the spin state of Ni^{2+} is due to the induction of tensile strain and unsaturated coordination defect. This is because active sites generally adsorb oxygen intermediates by hybridizing Ni 3d and O 2p orbitals. Hence, evaluating the orbital hybridization of Ni^{2+} in different spin states and of O* gives a good understanding of how this process is favourable. In the high-spin state of Ni^{2+} ($d_{z^2} = 1$), an unpaired electron occupying the d_{z^2} orbitals were present compared to the low-spin state ($d_{z^2} = 0$). Accordingly, due to spin–orbit interactions, the O* intermediates displayed energy level densities of 1.5 and 2 in the high-spin and low-spin states of Ni^{2+}, respectively. In particular, higher bond-order values and a lower-spin state of Ni^{2+} indicate enhanced interaction between active sites and oxygen intermediates, which favour OER activity.[52]

Shifts in lattice orientation can also modify the local environment of the active centre, which incorporates the positions and interactions of the coordination atoms. These adjustments can affect the distribution of electron spins and the organization of energy levels. Therefore, the spin state of electrons within the metal centre can be adjusted. Tong *et al.*[53] fabricated a $LaCoO_3$ thin film with multiple lattice coordination. Diverse crystallographic orientations of the electrocatalyst ensued in varying degrees of distortion in the CoO_6 octahedra, leading to a transition of the Co^{3+} spin state from a low-spin ($t_{2g}^6e_g^0$) to an intermediate-spin (IS) state ($t_{2g}^5e_g^1$). $LaCoO_3$ thin film acquiring (100) crystallographic coordination demonstrated the optimal Co^{3+} e_g orbital occupancy and the superior OER capability.[52,53]

DFT - lattice straining. Thse energy level changes induced by such strain can be modelled, and the resulting changes in spin state elucidated. For example, the decrease in ligand field splitting, as caused by tensile strain, stabilises higher spin states.

Li *et al.*[54] investigate how mechanical strain enhances the OER performance of two-dimensional cobalt oxyhydroxide (CoOOH). Through DFT simulations, they reveal that tensile strain induces a spin state transition in cobalt ions from low-spin to intermediate-spin and to high-spin which improves electron transfer and increases the number of active sites as seen in Fig. 2. This transition significantly lowers the overpotential required for OER, making the catalytic process more energy-efficient.

The study provides a mechanistic understanding of how strain affects the adsorption energies of key OER intermediates (OH, O, and OOH*), offering a new design strategy for electrocatalysts. They demonstrate that strain engineering is a scalable and effective method for tuning the electronic and magnetic properties of 2D materials, with broad implications for developing high-performance catalysts in energy conversion technologies.

Similarly, Wang *et al.*[55] used DFT to study how lattice strain affects the spin states of cobalt ions in $LaCoO_3$ (Fig. 3) and how this influences its catalytic activity. They found that when the material is stretched, the normal low-spin state becomes unstable and changes to an intermediate-spin state. In contrast, when the material is compressed, the low-spin state becomes more stable. Under tensile strain, the intermediate-spin state shows nearly full occupancy of the e_g orbital, which is known to be ideal for boosting oxygen redox reactions. This study clearly connects strain-driven spin changes to improved ORR/OER performance and shows that strain engineering is an effective way to control spin states and enhance oxygen electrocatalysis in perovskite oxides.

Defects and doping

The coordination structure of the active centres has a significant impact on the spin state. Both the coordination environment and the local electronic structure of the active centres are altered by the introduction of defects or doping atoms, a well-known strategy for reducing free energy barriers and creating new active sites.[20]

Doping can influence spin–orbit coupling, modifying the interaction between electron spin and orbital angular momentum. Based on the properties of doping species, doping can improve or hinder the magnetic properties of a material, and even absolutely alter the magnetic properties of the material.[56]

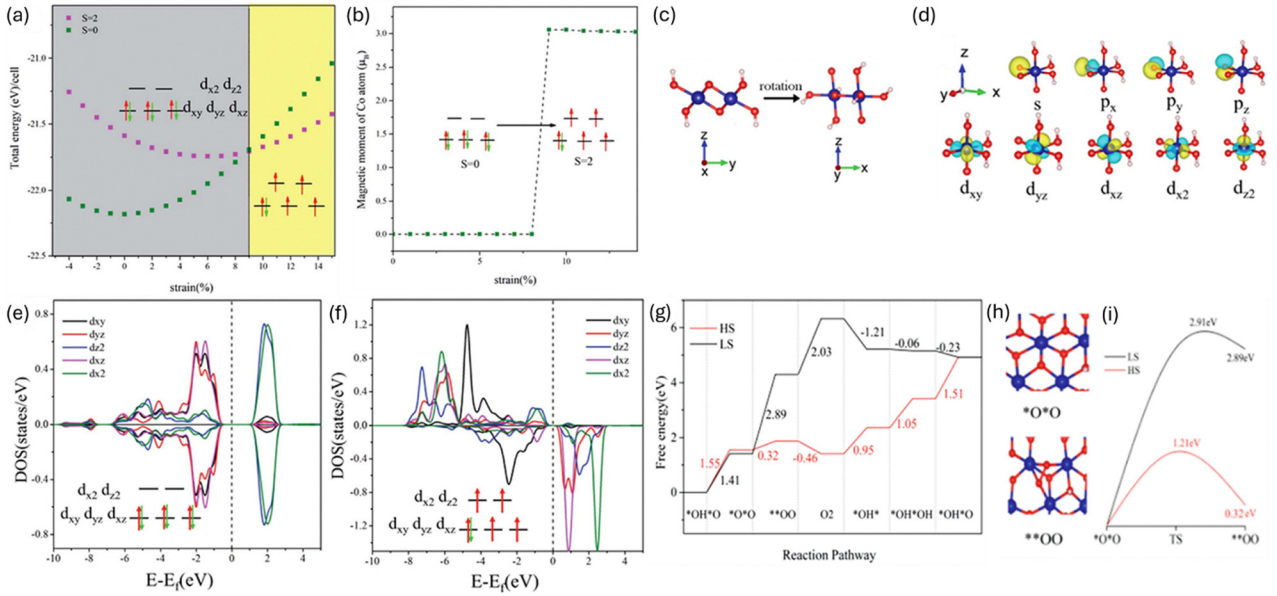

Fig. 2 (a) The total energy of CoOOH *versus* strain and (b) magnetic moment of Co^{3+} ions *versus* strain (c) Schematic rotation of CoOOH, (d) the calculated Wannier functions of Co 3d orbitals after rotation, and the PDOSs of Co 3d orbitals under a strain of: (e) 0% and (f) 9%. (g) The calculated free energy along the pathway for low-spin and high-spin CoOOH at U = 0 and pH = 0 through the intramolecular coupling mechanism, (h) the structural models of *O*O and **OO intermediates for the initial and final states of O–O coupling, and (i) the energy barriers for the O–O coupling on low-spin and high-spin CoOOH Reproduced with Permission.[54] Copyright RSC 2013.

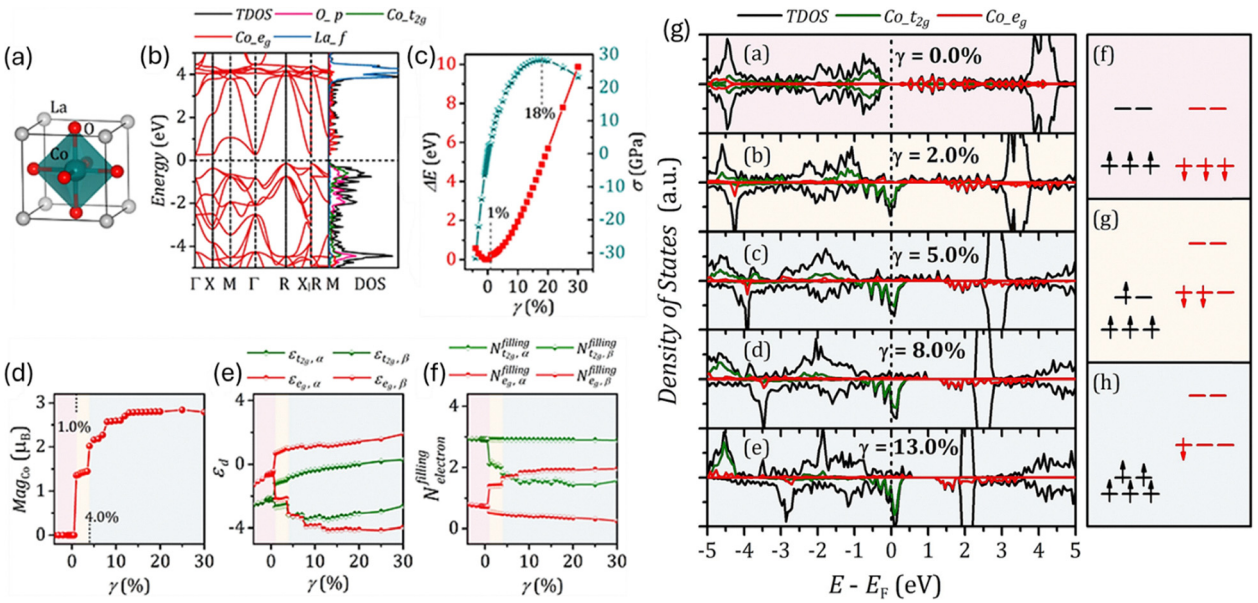

Fig. 3 (a) Crystal structure of $LaCoO_3$ and (b) corresponding band structure. (c) Strain energy of $LaCoO_3$ *versus* strain g and strain–stress curve, (d–f) Magnetic moment localized at Co atom (MagCo), d-band centre (+d), and d-band filling ($N^{filling}_{electron}$) *versus* strain γ. (g) DOS of $LaCoO_3$ under various strain: (a–e) g = 0.0, 2.0, 5.0, 8.0, and 13.0%. The schematic diagram of crystal field and corresponding spin arrangements: (f) low-spin, (g) intermediate spin, and (h) high-spin. Reproduced with permission.[55] Copyright 2020, Frontiers in Materials.

Spin state alterations can result from a variety of material defects. First, changes in spin–orbit coupling or local spin perturbations may arise from the introduction of new local electronic states or the modification of preexisting ones by defects. Likewise, the interaction amongst the defect and neighbouring electrons may lead to the spin localizations, or changes in spin coupling with other degrees of freedom, for instance charge.[8] Moreover, defects can induce local crystal structure transformations or distortions, which in turn can change the spin states of the electrons. For instance, reducing

catalyst size causes a multitude of defects, thus modifying the spin state of the active centre. The fabrication of γ-CoOOH nanosheet with a considerably large number of defects by reducing the γ-CoOOH thickness to 1.4 nm was a great achievement by Luo and Wu.[57] The manifestation of these flaws led to a transition in the spin state of the Co ion, transforming it from a low-spin state to a higher spin state. This transformation triggered a rearrangement of the Co 3d electrons, ensuing in the creation of $t_{2g}^5e_g^{1.2}$ arrangement.[57]

The γ-CoOOH nanosheet demonstrated outstanding OER activity due to the hypothetically optimal e_g orbital electron occupancy. At 10 mA cm^{-2} current density value, the overpotential of γ-CoOOH nanosheet was meaningfully lowered with 74 mV compared to the γ-CoOOH bulk, achieving 0.30 V. Furthermore, Pan *et al.*[58] prepared TiO_2 with special titanium defect concentrations controllably. The intrinsic relationship between electron spin polarisation and photocatalytic functioning was fully investigated. After the induction of titanium flaws, the spin-down polarisation of TiO_2-5 to TiO_2-10 near the Fermi level intensified. Though, too many titanium defects in TiO_2-20 and TiO_2-30 diminished the degree of spin polarisation. Novel findings exhibited that defect type $Ti_{0.936}O_2$ (TiO_2-10) with maximum spatial spin polarisation could successfully improve the charge separation efficiency and uphold the surface reaction process, demonstrating the best photocatalytic performance. In addition, the photocatalytic activity of spin-polarized $Ti_{0.936}O_2$ could be further enhanced by external magnetic field.

DFT - defects. The enhancement of ferromagnetic character can also be seen through computation. A spin-polarisation-mediated approach to improve OER activity in acidic electrolytes through doping dilute manganese (Mn^{2+}) (S = 5/2) in antiferromagnetic RuO_2 to produce a net ferromagnetic moment was reported by Li *et al.*[23] When Mn was put into RuO_2 lattice, its magnetic form transformed. The doped Mn atom had a large magnetic moment (~3.69) and induced a ferromagnetic arrangement of the magnetic moments of closest Ru atoms. Mn–RuO_2 nanosheets presented OER activity improved by a strong magnetic field, showing a minimum overpotential of 143 mV and preserving higher activity for 480 hour without any substantial reduction.[8,23]

Likewise, the introduction of heteroatoms not only changes the magnetic properties of the catalyst but also directly influences the spintronic arrangement of the metal centre. A bimetallic atom-dispersed electrocatalyst (Fe, Mn/N–C) was demonstrated by Yang *et al.*[59] that Mn–N distributed by neighbouring atoms could successfully activate the Fe^{3+} site, allowing Fe^{3+} to attain a single e_g electron filling ($t_{2g}^4e_g^1$) in the FeN_4 spot, which was extra conducive to electrons entering the antibonding orbital of O then realizing the activation of O_2. According to magnetic susceptibility measurements, it was observed that Fe/N–C encompassed nearly 1.3 unpaired d electrons. This implies that the Fe^{3+} ions in Fe/N–C show a low-spin state with no e_g filling. On the contrary, the amount of unpaired d electrons of Fe, Mn/N–C was about 3, revealing single e_g filling. Hence, the adjacent Mn^{3+} moieties in a low-spin state allow Fe^{3+} in FeN_4 to accomplish the anticipated e_g filling, ensuing the most favourable electronic configuration. This arrangement leads to remarkable ORR activity and stability of Fe, Mn/N–C in both acidic and alkaline media.[59]

Fang *et al.*[60] developed a new method to improve the OER by adjusting the secondary coordination sphere (SCS) in Fe-doped $LaCo_{1-x}Fe_xO_3$ perovskites. This adjustment helped stabilize the intermediate-spin state of cobalt ions. Controlling the spin state enhanced orbital interactions and charge transfer during the OER process.

DFT calculations supported these results by showing how changes in the SCS affected the electronic structure. The DFT results revealed that the IS state reduces the energy barrier for O–O bond formation, speeding up the reaction. As shown in Fig. 4, the schematic of spin-state control and the DFT-based energy profiles clearly demonstrate how SCS engineering affects spin energetics and reaction pathways.

These findings highlight the power of DFT in explaining and predicting spin-related catalytic behaviour. Building on this idea, our review discusses how DFT-guided spin control strategies can be applied to both the ORR and the OER, providing a unified understanding of the relationship between spin states and electronic structures in electrocatalysis.

Contrasting results were found when Zheng-Da He *et al.*[61] used DFT and thermodynamic modelling to study the spin state of Fe in Fe-doped NiOOH electrocatalysts. They found that at low doping levels, Fe prefers a low-spin configuration with a magnetic moment of about $0.2\mu_B$, compared to around $3.7\mu_B$ for the high-spin state. This low-spin state is more stable by about 0.5 eV per Fe atom and allows high Fe solubility, up to 25% substitution, without causing structural distortion. The calculated Fe–O and Ni–O bond lengths are both close to 1.90 Å, matching experimental results. The presence of low-spin Fe improves the electronic conductivity of NiOOH and promotes faster charge transfer during the OER. In addition, Fe doping lowers the OER overpotential by stabilizing key intermediates such as *O and *OOH, reducing the reaction energy barriers. It should be noted here that the iron does not serve as an active site, but to enhance conductivity. The lesson is clear: high spin state in the overall material should not be a goal in itself. Unpaired electrons are most useful at the reaction site, and may in fact be detrimental in the bulk material.

This is well demonstrated by Wan *et al.*[62] using a series of single-atom catalysts (SACs), including Ni-CNG, Co-CNG, and Fe-CNG, along with a dual-atom NiFe-CNG system, all supported on graphitic carbon nitride (g-C_3N_4). To probe the electronic structure and catalytic behaviour of these materials, they employed spin-polarized DFT calculations. As shown in Fig. 5, the spin density analysis (Fig. 5b) revealed that Ni atoms consistently exhibited a low-spin configuration, while Fe atoms adopted a high-spin state, characterized by unpaired electrons in both the t_{2g} and e_g orbitals. This spin asymmetry was especially pronounced in the dual-atom NiFe-CNG system, where the *in situ* formation of Ni–O–Fe bridges created a unique electronic environment. The spin disparity between Ni and Fe facilitated directional electron transfer during the OER,

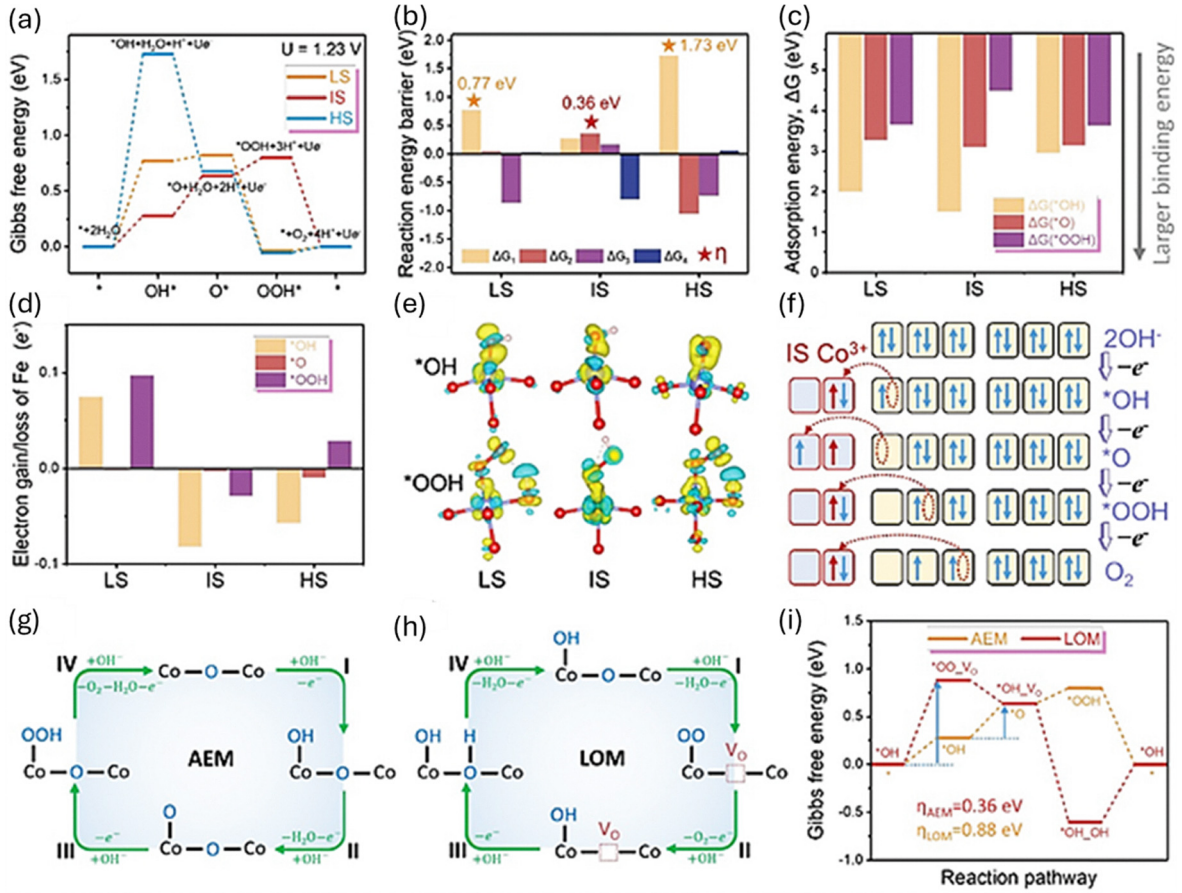

Fig. 4 The theoretical OER activity of the $LaCo_{1-x}Fe_xO_3$ with different spin state (low, intermediate and high-spin, LS, IS and HS, respectively). (a–d) Gibbs free energy diagram, reaction energy barrier, adsorption energy and electron gain/loss after the adsorption of oxygen intermediate at different Co active site of $LaCo_{1-x}Fe_xO_3$ with different spin state during OER process. (e) Different charge density of $LaCo_{1-x}Fe_xO_3$ with different spin state before/after the adsorption of *OH and *OOH. (f) Four spin electron behaviours on IS Co^{3+} during the triplet O_2 generation process. (g and h) Schematic diagram of AEM and LOM mechanism. V_O represents the vacancy of lattice oxygen. (i) Gibbs free energy diagram at IS Co site in $LaCo_{7/9}Fe_{2/9}O_3$ for OER process with AEM and LOM mechanism. Reproduced with permission.[60] Copyright 2024, Wiley-VCH.

establishing effective spin-polarized channels that enhanced catalytic performance.

DFT simulations further revealed that the local electronic structure of NiFe-CNG was optimized to support cooperative interactions at the Ni–O–Fe interface. The DOS plots (Fig. 5c) showed enhanced orbital overlap and charge delocalization compared to single-atom counterparts, while the free energy diagrams (Fig. 5a and d and e) demonstrated reduced energy barriers for OH^- adsorption, O_2 release, and the RLS of the OER. These findings culminated in a proposed OER pathway (Fig. 5f), where unobstructed spin channels within the Ni–O–Fe bonds significantly augmented the adsorption energies of key intermediates and facilitated efficient multi-electron transfer. Collectively, these DFT insights underscore the importance of spin state modulation, electronic structure tuning, and dual-site synergy in designing high-performance oxygen electrocatalysts.

Table 3 shows a comparison of analogous systems' electrocatalysis in different spin states. Through the following sections we will show the next generation spin control, where both spin state and spin-direction correlations are parameters open to electrochemists.

Magnetism

Historical context

In the 19th century, Maxwell proposed that electricity and magnetism were manifestations of the same "electromagnetic" force, mediated by electromagnetic waves called photons, and the two were unified by the famous Maxwell equations. Magnetism on macroscopic scales can generally be described either as a relativistic phenomenon emerging from the movement of charge, such as electricity through a wire, or due to the alignment of electron spins as in a permanent magnet. In either case, a magnetic dipole is produced, with a north and south pole. Historically, the most important magnetic phenomena on earth arose from the planet's own vast magnetic field, due to the movement of molten material in the core. This magnetic field deflects charge particles emitted from the sun, protecting life from this deadly radiation. The planetary

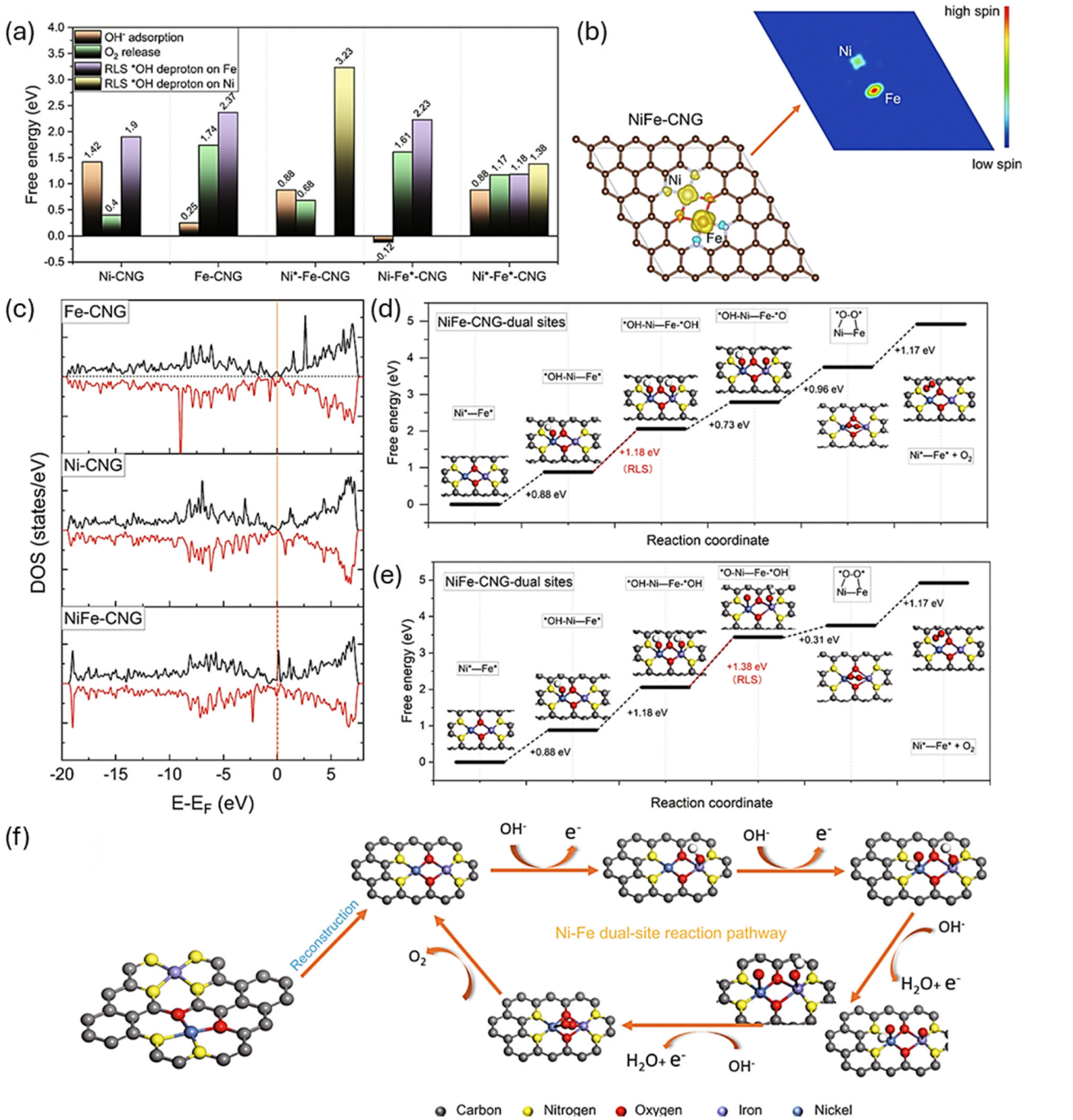

Fig. 5 DFT simulations and proposed OER pathways. (a) Free energy comparison of OH− adsorption, O_2 release, and the rate limiting step (RLS) between different structural configurations. (b) Spin density pattern (left) and spin channel (right) of Ni and Fe sites in NiFe-CNG. The isosurfaces in yellow and blue represent spin-up and spin-down densities, respectively. (c) Density of states (DOS) of Fe-CNG, Ni-CNG, and NiFe-CNG. (d) and (e) Free energy diagrams of NiFe-CNG models toward OER at the Ni-Fe dual site. (f) Schematic illustration of the proposed overall OER pathway for the NiFe-CNG catalyst. Reproduced with permission.[62] Copyright Nature 2021.

magnetic field also interacts with permanent magnets, as discovered by ancient Greeks and Chinese philosophers. The ''lodestone'' typically iron oxide as magnetite ore, tended to align with the planetary magnetic field. This phenomenon was used for ceremonial purposes, and eventually for navigation: magnetic north could be found even when conditions did not permit navigation by the sun or stars.[65] Perhaps, like those historical navigators, we may use the tendency of small magnetic dipoles to align with a magnetic field to chart a course towards rapid and efficient electrocatalysis.

Magnetic enhancement mechanism

The use of magnetic fields in catalysis is itself a growing field of study, with three main contributing effects: (i) modulation of

Table 3 Activities of changing spin systems for OER and ORR

Active metal	Material	Spin state	$E_{1/2}$/V *vs.* RHE	$E_{j=10}$/V *vs.* RHE	Ref.
Iron	Fe-N_4	Low-spin Fe^{2+}	0.80	—	63
	Fe-N_4	Intermediate spin Fe^{2+} and Fe^{3+}	0.89	—	
	Fe-N_4 + Cu-N_4	Intermediate spin	0.85	1.56	31
	Fe-N_4 + Cu-N_4	High-spin	0.86	1.54	
Cobalt	Co_3O_4	Lower (XAS estimate)	—	1.57	64
	Co_3O_4-50 (defect rich)	Higher (XAS estimate)	—	1.51	
	Co_3O_4	2.85μ_B	0.77	—	49
	Ni doped Co_3O_4	2.99μ_B	0.84	—	
Nickel	NiOOH	0.310μ_B	—	1.53	50
	NiOOH heterojunction	0.613μ_B	OCV of 1.56 in zinc-air battery	1.50	

electron spin and atomic spin states, improving the electron transfer kinetics (ii) magnetohydrodynamic (MHD) effects which boost mass transfer processes in the electrolyte (iii) magnetothermal effects, whereby localised heating speeds conversion in an energy efficient way and without placing the rest of the system under thermal stresses.[66]

The spin effect may be studied in isolation as it is the only magnetic influence on charge transfer in a static field - magnetothermal effects require an alternating magnetic field (AMF), while Lorentz and Kelvin forces impact mass transport.[67] The high-spin state is stabilised by application of an external magnetic field. The unpaired electrons then align parallel with the field, lowering the energy of the system.[21,66,68]

Hysteresis loops are frequently used to confirm ferromagnetic character, but the shape of the loop—specifically coercivity and remanence—represents an underutilised design parameter. Materials with high remanent magnetisation could theoretically sustain spin-polarisation without external fields, simplifying device architecture by removing the need for permanent magnets in the electrolyser stack. Conversely, tuning the area of the hysteresis loop is critical for AMF-assisted catalysis; minimising the loop area is necessary to decouple pure spin-polarisation effects from magnetothermal heating. Future design strategies should therefore focus on 'hysteresis engineering' alongside simple composition tuning.

In transition metal catalysts, fundamentally, the spin state of the active metal centre is a descriptor for catalytic performance in OER/ORR electrocatalysis[69] as explored earlier in this review: the active centre magnetic moment ranges from higher magnetic moment which correlates to a high-spin state, to low magnetic moment which correlates to low-spin state.[70] Therefore, except for the induced mass transfer effects associated with Kelvin and Lorentz forces, the spin state changes induced by magnetic fields and other spintronic effects can be linked to activity enhancements on these materials. Studies have shown that in the ORR process, applying a magnetic field significantly impacts paramagnetic oxygen molecules leading to an increased electron transfer process. Similarly, in the OER process, external magnetic field enhances the parallel alignment of oxygen radicals resulting in improved activity.

Magnetic enhancement in catalysis

Such magnetic field treatment technique can be used to inspect and understand the underlying mechanisms of spin-related incidents. The magnetic field has an important role in spin control, with considerably improving spintronics. Zhang *et al.*[8] used carbon nanofiber/cobalt sulphide (CNF/CoS_x) *via* the electrospinning of polyacrylonitrile/cobalt (PAN/Co) fibres, following carbonization and lower-temperature vulcanization.[8,71] The external magnetic field caused Co to transition from low-spin to high-spin state conditions, resulting in extra unpaired electrons in Co 3d orbital. The spin polarisation controls the chemical adsorption, band gap, and charge transport properties of the catalysts. The spin density of Co atom in the CoS_2 was evenly allocated in the absence of an external magnetic field. The occurrence of an external magnetic field caused the alignment of electron spins. From the estimated state density, after spin polarisation, the overlap of Co 3d orbitals with S 2p orbitals improved, developing a powerful 3d–2p hybrid orbit. The development of 3d–2p hybridization, driven by formation of ligand holes, assisted the dynamics of charge transfer at the interface. By the principle of spin angular momentum conservation, there is a likelihood of electron–electron repulsion among the catalyst and sulphur-adsorbing species. So, this interaction can improve conductivity, lower the energy barrier of the electrochemical reaction, and improve the kinetics of the Li–S reaction process.[72]

The implementation of ferromagnetic ordered catalysts for spin polarisation with a magnetic field to promote the OER was reported by Ren *et al.*[21] Primarily they examined the magnetic properties of $CoFe_2O_4$, Co_3O_4, then IrO_2. The hysteresis loop results proved that $CoFe_2O_4$ revealed ferromagnetic characteristics at room temperature, but Co_3O_4 and IrO_2 showed antiferromagnetic or paramagnetic characteristics at room temperature, correspondingly. The OER performances of electrocatalysts with various magnetic properties were examined with and without application of a constant magnetic field of 10 000 Oe. The OER properties of ferromagnetic $CoFe_2O_4$ were shown to be improved, but the changes in nonferromagnetic Co_3O_4 and IrO_2 were not significant. Ferromagnetic $CoFe_2O_4$ could accelerate the OER *via* spin polarisation and fast spin-electron exchange with adsorbed oxygen. The outcomes demonstrated that the Tafel slope of $CoFe_2O_4$ transformed from $\sim$120 mV dec^{-1} to $\sim$90 mV dec^{-1} after the magnetic field application.[21] This showed that the rate-determining step (RDS) of the OER process under the external magnetic field had altered from the first electron transfer step to a mixed RDS including the first electron transfer step and second steps;

revealing, the first electron transfer step was no longer the RDS. By the principle of spin angular momentum conservation, the exchange of spin-polarized electrons between $CoFe_2O_4$ and the adsorbed oxygen or the reactant resembled ferromagnetic exchange, leading to improved reaction kinetics for the first electron transfer. But this phenomenon was not shown on nonferromagnetic electrocatalysts.[73]

For electrochemical settings, surface treatment of the electrocatalyst often done to produce the active constituent. And so, the control of the magnetic substrate and active surface area by renovation is also a vital approach to develop efficient spintronic electrocatalysts. In $ZnFe_{2-x}Ni_xO_4$, the number of Ni^{3+} ions were used to control the specific coordination environment, thus enabling the *in situ* construction of highly active electrocatalytic species through surface reconstruction and construction of a ferromagnetic core to favour spin-selective electron transfer as demonstrated by He *et al.*[74] Integrating 20 percent of Ni^{3+} results in the *in situ* formation of a paramagnetic FeNi(oxy)hydroxide catalytic layer on the ferromagnetic $ZnFe_{1.6}Ni_{0.4}O_4$ core during OER process analysis. The formed catalytic active layer sped up the OER kinetics, revealing a lower overpotential of 360 mV at a current density of 0.5 mA cm^{-2}, showing superior activity over the benchmark IrO_2 at 420 mV. The activity can also further be increased by nearly 2.9 times by employing an external magnetic field, surpassing $ZnFe_2O_4$ by a factor of 39 at an overpotential of 350 mV. This boost is attributed to the promoted spin-selective electron transfer aided by ferromagnetic exchange interaction, that penetrates through the paramagnetic reconstruction layers. This research work by He *et al.* offers a novel method to develop highly efficient catalysts *via* the coupling of ferromagnetic ordering channels and highly active catalytic species.

Similarly, Jiang *et al.*,[76] taking advantage of the spin polarisation of ferromagnetic materials in the presence of a magnetic field, studied the effect on the OER catalytic activity of amorphous FeNiCo-based catalyst tailored by Cr, Nb, and Mo. The study revealed modulation of the local atomic structure of the strongest ferromagnet, FN-Nb material, with a higher coordination number of Fe clusters compared to FN-Mo and FN-Cr with low coordination number of Fe clusters, in the presence of an external magnet causes spin polarisation of the electrons and resultant enhancement of the OER kinetics which leads to a decrease in overpotential and Tafel slope. The FN-Nb revealed a decrease exceeding 20 mV with a current loading of 100 mA cm^{-2} and a 65.2% increase in the turnover frequency (TOF). A novel "mixed-valent cobalt modulation" strategy was employed to enhance oxygen electrocatalysis in perovskite $LaCoO_3$ (LCO) oxide by Wang and co-workers.[75] Modulation of the oxidation state of cobalt ions to induce magnetic properties in the LCO was achieved through an ethylenediamine (EDA) post reduction procedure at ambient temperature. The crystal structure and phase information of the as-synthesized LCO catalyst was done using PXRD technique (Fig. 6a) while SEM, TEM, HRTEM and High Angle Annular Dark Field STEM

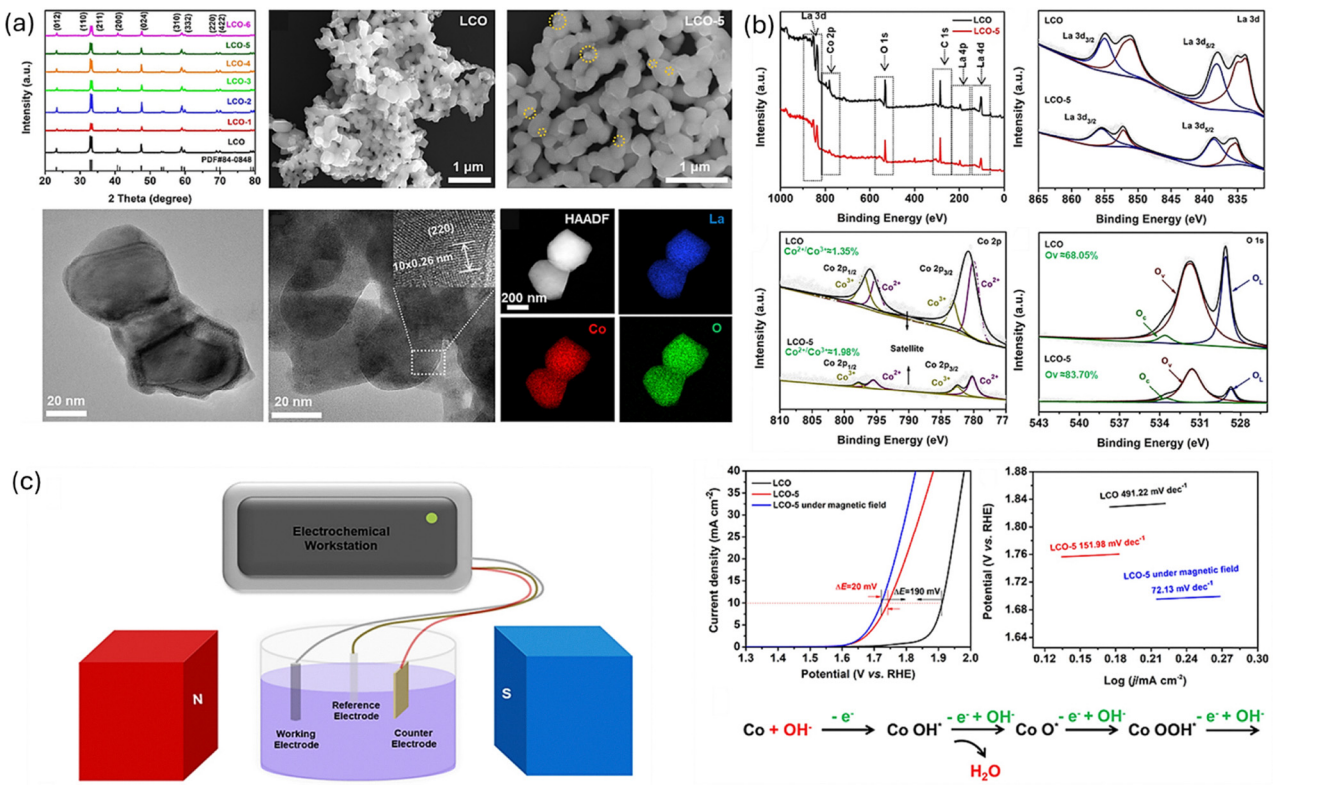

Fig. 6 (a) Crystallinity and morphology of LCO and LCO-X were determined by XRD, SEM, TEM, HRTEM and HAADF-STEM; (b) Survey spectra and chemical states of the elements by XPS spectra, OER linear sweep voltammetry, and Tafel plots; (c) Schematic of the experimental set-up for the magnetic field enhanced electrocatalysis. Reproduced with permission.[75] Copyright Wiley 2022.

(HAADF-STEM) analysis was done to determine their morphology. The optimized LCO-X with Co^{2+}/Co^{3+} ratios increased by about 1.98% compared to the pristine LCO as seen in the XPS analysis (Fig. 6b). This unique property endowed enhanced OER activity with benchmark potential at 10 mA cm^{-2} decreased by 170 mV compared to the pristine. Furthermore, the ferromagnetic LCO catalyst under an external magnetic field revealed a further decrease in the overpotential at 10 mA cm^{-2} by 20 mv compared to the analysis under zero magnetic field (Fig. 6c and d). The enhanced electrocatalytic performance can be ascribed to increased energy states of electrons of the LCO induced by the external magnetic field.

Reporting in a review article, Fang *et al.*[41] summarized recent progress and advances on the effects of spin-modulation on oxygen electrocatalysis of magnetic transition metal catalysts (TMCs). Owing to the spin state interconversion between the singlet OH^-/H_2O and triplet O_2 which is forbidden due to the need for spin flipping, hence, the spin of TMCs affects significantly the kinetics of OER/ORR and therefore the overall performance. The review emphasized the importance of spin states (e_g filling) as an important descriptor to explain and improve OER kinetics because $e_g \sim 1.2$ represents optimal interaction (*i.e.* modulates adsorption/desorption energies) between oxygen intermediates and catalytic active surface areas in the TMCs. The e_g filling can be modulated in two ways (i) on the atomic/electronic scale: whereby the crystal field and oxidation states of active-site ions is altered, (ii) on the microscale by tailoring desired morphology and nanostructure of TMCs. The authors revealed that besides the spin-states regulation, the transfer of $4e^-$ during the OER/ORR process can be optimized through construction of spin selective channels that allow only electrons with the same spin to cross. In this regard, the intricate interplay between spin and magnetism plays a vital role in facilitating the spin polarisation, enhancing the filtration and transfer of spins with the same direction for the generation/conversion of triplet ↑O═O↑. An integrated magnetic field was employed to manipulate the spin of heterogenous nitrogen-coordinated single metal atom (M–N–C) for the oxygen reduction and oxygen evolution reactions (OER and ORR) by Yu *et al.*[66] This study revealed that the spin states of the catalytic active sites can be manipulated without altering their atomic structure. Using experimental controls, the study revealed the catalytic performance improvements did not emanate from magnetic Lorentz and Kelvin forces but solely to the built-in magnetic field with potential to promote low-spin to high-spin transition in the Co active site of the CoPc. Using molecular orbital interaction and density functional theory (DFT) calculations, the authors revealed the stabilization of the *OOH intermediate and facilitation of H_2O_2 formation by the high-spin-Co site. The built-in magnetic field can also facilitate the alignment of electron spins to enhance favourable spin transitions during OER, leading to overcoming the kinetic barrier associated with doublet *OH to triplet O_2 transitions.

The responsiveness of electrocatalysts to optical–magnetic coupling technology is vital for effective and comprehensive enhancement of overall catalytic performance. In this regard, Wang *et al.*[77] reported on the synthesis of crystalline iron hydroxides anchored on a nickel foam the $Fe(OH)_x$/NF (M, 0 °C) through a facile low-temperature magnetic field-assisted electro-deposition method. X-ray photoelectron spectroscopy was used to determine the chemical nature of the catalyst materials, the M^{2+} and M^{3+} states were predominant with the presence of oxygen vacancies associated with defects. The effect of the external magnetic field enabled hole and electron transfer during the electrocatalytic process (Fig. 7), improving the OER performance as exemplified by reduction of the overpotential at 10 mA cm^{-2} which were previously around 285 and 222 mV to about 63 mV, as well as improved stability. The superior performance of the $Fe(OH)_x$/NF(M, 0 °C) to those synthesized *via* conventional electrodeposition methods is ascribable to the directed carrier (hole and electron) transfer effect enabled by the highly crystalized $Fe(OH)_x$ and ferromagnetic nickel foam.

The surface reconstruction of electrocatalysts to achieve efficient water oxidation is quite challenging due to the complex reaction conditions. Herein, Ma *et al.*[78] designed and

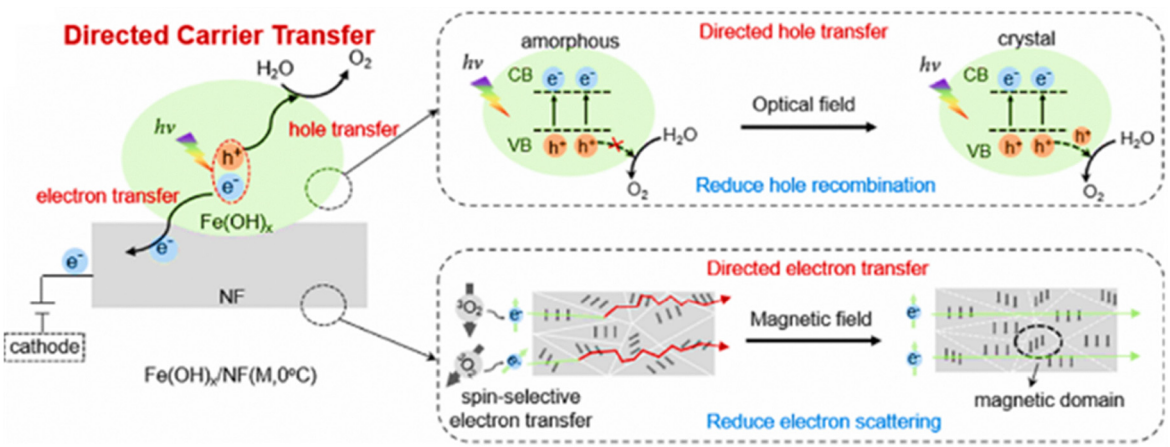

Fig. 7 Schematic illustration of the effects of directed carrier transfer in the presence of magnetic and optical field during the OER electrocatalysis using $Fe(OH)_x$/NF(M,0 °C). Reproduced with permission.[77] Copyright ACS 2024.

synthesized a core–shell CFO@CoBDC ferromagnetic/paramagnetic composite following a two-step procedure: (i) $CoFe_2O_4$ (CFO) core was synthesized *via* sol-gel method and (ii) modification of the CFO to CFO@CoBDC was achieved *via* a solvothermal method. The surface reconstructed catalyst CFO@CoBDC was investigated for oxygen electrocatalysis in alkaline electrolyte medium under the influence of gradient magnetic field. The study revealed that Kelvin force from the core's local gradient magnetic field influences the electrochemical surface reconstruction of the shell, leading to a higher proportion of Co^{2+} on the catalytic active sites. The prevalence of Co sites with optimized electronic configuration which was observed though DFT calculations results in favourable adsorption energy for oxygen-containing intermediates, hence lowered activation energy for the electrocatalysis. Therefore, improved OER performance was observed with the overpotential reduced to 28 mV at benchmark current density of 10 mA cm^{-2} and larger current density at 1.63 V. The overall OER performance recorded in this study is ascribable to spin modulation of the surface electrons of the surface reconstructed CFO@CoBDC in the presence of a gradient magnetic field. The intrinsic correlation between magnetic nanocatalysts and external magnetic fields boosts electrochemical performance; this was explored by Chen *et al.*[79] in the rational design of magnetic nanocatalysts Mn–Co–Fe oxide which was obtained by doping Mn and Co into the spinel structured F_3O_4 following a hydrothermal route and the products are named MCF1, MCF2 and MCF3. The as-synthesized nanocatalysts with adjustable magnetic properties in the presence of an external magnetic field showed the paramagnetic oxygen molecules experience a Kelvin force, while the Li^{2+} ions experienced a Lorentz force. The influence of these two magnetic forces accelerates diffusion, hence an improved OER/ORR kinetics and reduced overpotential. Therefore, an increase in specific capacity of up to 52.9% was recorded and a notable 108 mV reduction in overpotential. The changes in the performance of lithium-ion batteries were studied by Comsol Multiphysics simulation and DFT calculations, results point to lowering of the energy barrier for the formation and decomposition of Li_2O_2 under the influence of a magnetic field. The generation of a high energy N atmosphere was achieved by plasma to enable bonding of Fe cations onto CoO through the N-channel to form N–Fe–CoO nanoarrays. Huang and co-workers,[80] observed that the coupling of N and Fe co-doping causes a decrease in electron density around the Co^{2+} centres, a phenomenon which not only increases the unpaired electrons for electron acceptors but also amplifies the magnetic enhancement effect. The conditions lead to improved OER performance under a parallel magnetic field with 420 mT intensity, hence, the lowering of the overpotential and Tafel slopes to 217 mV and 25.1 mV dec^{-1} respectively. The improved OER electrocatalysis can be ascribed to magnetohydrodynamic effect which causes both increased mass and charge transfer phenomena, hence, lowering the escape energy barrier reduction of the paramagnetic triplet state O_2. The findings in this study highlight a scalable pathway for coupling heteroatoms with magnetic field which provides solutions to some of the bottlenecks causing poor performance of non-noble metal electrocatalysts.

Vensaus *et al.*[81] report a similar finding for ORR, where the closer a silver surface was to a permanent magnet, the greater the enhancement in ORR current and onset potential. There was a significant decrease in current response when the silver layer was thicker than 100 nm, which the authors attributed to loss of spin polarisation due to interaction with the non-magnetic silver lattice. Their experimental setup was interesting, having electrons first be conducted through the magnet before reaching the catalyst layer. This was done to separate spin polarisation from magnetohydrodynamic effects, but also shows a possible path to incorporating magnetic materials as structural parts of an electrochemical reactor, such as current collectors in this case.

In a study by Zhu *et al.*,[82] the controversy around the source of magnetic-induced heating (MIH) effects was explored to ascertain if the source is from the catalysts or from the current collectors. This is also to ascertain the source of catalytic performance associated with MIH effects. Herein, Zhu and co-workers designed a revised three-electrode system that is free from interferences from magnetothermal effect, ensuring the MIH effects originates from the composite electrocatalysts $Ni@Ni(OH)_2$ and $Ni@Ni_2P$ with core–shell morphology. The core–shell structured heterojunction ensures rapid response to the heat generated from the ferromagnetic Ni cores, therefore in an alternating magnetic field (AMF) activity enhancement is guaranteed. Hence, in the presence of a 60 mT AMF, the as-synthesized catalysts $Ni@Ni(OH)_2$ and $Ni@Ni_2P$ showed identical performance improvements in OER and HER, an indication that the MIH effect is uniform in its enhancement of the rate of catalysis. With the more representative $Ni@Ni(OH)_2$ showing good stability of over 10 h and an OER overpotential of 384 mV at 50 mA cm^{-2} in the presence of 60 mT AMF, superior to traditional industrial operating temperature of 80 °C. Though not a spin polarisation effect, the innovative findings by the authors pave the way for the application of AMF to non-magnetothermal catalysts, broadening the horizon for the development of AMF-assisted new catalysts.

A static external magnetic field was employed to enhance the oxygen electrocatalysis of high-entropy spinel oxide $(CuCoFeMnNi)_3O_4$ (HESOx) by Hechter *et al.*[83] The $(CuCoFeMnNi)_3O_4$/C synthesized by the Pechini method was characterized by synchrotron powder X-ray diffractograms (PXRD) to show the possible 5 cation substitution in the octahedral and tetrahedral sites and the resultant or total inversion of the structure as well as two different spinel-type structures, as illustrated in Fig. 8.

The spinel structure of the HESOx showed distorted O^{2-} lattice indicating defects with majority of the metals existing in the M^{2+} and M^{3+} states as well as ferromagnetic characteristics. These properties bode well for improved electrocatalytic performance and as recorded by the authors, the composite exhibited OER/ORR catalytic activity comparable to state-of-the-art bifunctional catalysts with ΔE = 0.65 V (bifunctionality index) and superior to commercial IrO_2 in OER recording a

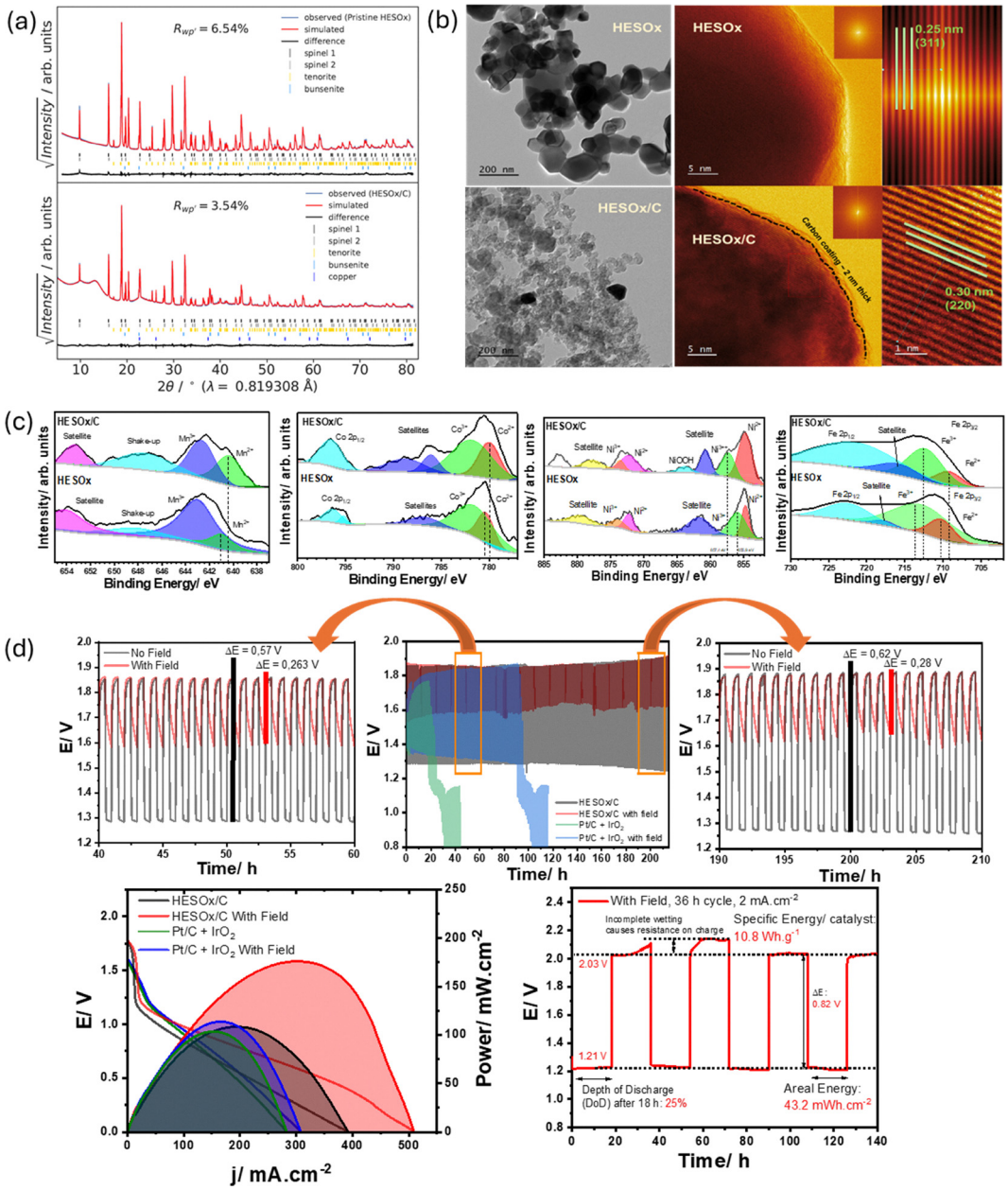

Fig. 8 Crystallinity and phases of the HESOx was determined by synchrotron powdered X-ray diffraction (a); TEM and HRTEM micrograph of HESOx and HESOx/C crystal with lattice planes and lattice parameters (b); Analysis of the chemical states and composition of the elements by XPS (c) and (d) results of the RZAB tests with/without an external magnetic field. Reproduced with permission.[83]

potential at the benchmark current density of 10 mA cm^{-2} (E_{j10} = 1.534 V). The improved performance can be ascribed to increased surface area, surface oxygen defects with associated reaction electrons associated with material morphology while the enhanced conductivity and reaction kinetics is due to spin electron modulations by an external magnetic field. The effect of the external magnetic field was also recorded by the authors in the RZAB tests with the peak power increasing from 101 mW cm^{-2} without an external magnetic to 169 mW cm^{-2} in the presence of an external magnet. The effect of the magnetic field was also recorded in the RZAB stability test with the composite HESOx achieving discharge/charge cycles of over 140 h with an areal-discharge energy of 43.1 mWh cm^{-2} according to Fig. 8 d. The authors briefly note that improved power profile persists even after the magnetic field is removed, indicating that the catalysts themselves had been magnetised. The result of this work reinforces the appeal of high-entropy spinels in electrocatalysis and application of a static magnetic field as a viable approach to enhance activity.

Some further examples of magnetically enhanced catalysts are listed in Table 4. It is once again interesting that the use of a "residual" magnetism by Zhang *et al.*[84] led to improved performance. If the magnetic field and spin polarisation can be entirely supplied by the catalyst or substrate itself, magnetic

Table 4 OER and ORR parameters for magnetically enhanced catalysts

Catalyst	Magnetic field/mT	OER E_{10}/V	ORR $E_{1/2}$/V	ΔE/mV	Ref.
Co/CNF	0	1.650	0.800	850	66
	350	1.635	0.820	820	
$FeCo_2O_4$ nanofiber	0	1.580	—	—	85
	1000	1.540	—	—	
$FeCo_2O_4$	0	1.58	0.78	800	84
	Residual	1.52	0.80	720	
$Ni_{1.5}Co_{1.5}O_4$/Ni foam	0	1.520	—	—	86
	125	1.478	—	—	
(Fe + N + S)/C	0	—	0.88	—	87
	140	—	0.91	—	
(Ru-Ni)O_x@NF	0	1.583	—	—	88
	400	1.516	—	—	

enhancement on a practical device scale becomes truly feasible. Magnetising materials during manufacturing is far less daunting than designing devices that include a complex electromagnet or expensive permanent magnet.

DFT - magnetic field

Ren *et al.*[89] used spin-polarized DFT to study how magnetic fields affect the OER on ferromagnetic catalysts. Their simulations showed that magnetic ordering creates a difference between spin-up and spin-down electrons. This helps align the electron spins with the natural triplet state of oxygen molecules, which lowers the energy needed for the first electron-transfer step. Fig. 9 in their paper shows the spin-resolved DOS and free-energy diagrams, clearly indicating that magnetic fields stabilize spin-polarized states and reduce reaction barriers compared to non-ferromagnetic systems.

They also analysed the adsorption energies of key OER intermediates (*OH, *O, *OOH). The results showed that magnetic spin alignment greatly reduces the Gibbs free-energy barrier for forming *OOH, which is often the slowest and rate-limiting step. When they compared ferromagnetic and non-ferromagnetic catalysts, they found that only ferromagnetic materials benefit from magnetic spin polarisation, while non-ferromagnetic catalysts show almost no change.

These findings from Ren *et al.* show that magnetic spin alignment speeds up O–O bond formation and enhances catalytic activity, offering useful guidance for designing future spin-engineered catalysts for water electrolysis.

Characterisation

Magnetic ordering in materials is a well-developed field and has been studied by a variety of methods such as magnetoresistance and neutron scattering. More recently, resonant inelastic scattering (RIXS) and X-ray absorption experiments offer a closer look at local magnetic ordering.[90,91] While powerful, such techniques are often unsuited for *operando* experiments needed to truly follow the role of magnetism in the oxygen reactions. *Operando* X-ray Magnetic Circular Dichroism (XMCD), however, is a technique that enables the direct measurement of spin polarisation and magnetic order, demonstrating how CISS aligns spins to overcome spin-forbidden steps in O_2 evolution/reduction. For example, magnetically tuned XMCD for spintronic interfaces reveals spin state roles in OER.[92]

Chiral spin selection effect (CISS)

Historical context

The study of chirality began with the discovery of polarized light by *Étienne-Louis Malus* in 1808.[93] Following his work, Arago and Biot investigated how certain crystals and organic substances interact with polarized light. Arago observed that quartz crystals could produce two coloured polarized images when viewed with an Iceland spar analyser. While Biot conducted the definitive experiments, finding that quartz rotated the plane of polarized light at an angle proportional to the crystal's thickness, with the rotation angle differing for each colour. Crucially, Biot also discovered that many organic substances like sugar, turpentine, and camphor solutions rotated polarized light either to the left or right, suggesting the origin of this property was not just crystalline but molecular.[93] In 1820, John Herschel linked this optical activity to the macroscopic structure of crystals, linking the direction of rotation (right or left) in quartz to the handedness of its crystal faces, known as plagihedrals as seen in Fig. 10.[93]

In early 1820, dissymmetry was used in the French language to describe the disruption or absence of symmetry, or dissimilarity or difference in appearance between two objects.[94] A breakthrough from Louis Pasteur occurred in 1848, proving that chirality was molecular, not just crystalline, while observing crystals of sodium-ammonium tartrate and paratartrate, he noticed that the paratartrate existed as two types of crystals whose faces were oriented either to the left or the right.[95] By manually separating the mirror-image crystals with tweezers, Pasteur proved that the chemically identical paratartrate was actually a racemic mixture of two enantiomers.[93] This demonstrated that molecular structures could exist as non-superimposable mirror images, laying the foundation for ''geometrical chirality''.[94,96,97]

The philosophical understanding of handedness was first addressed by Immanuel Kant in his 1768 paper, where he introduced the term ''incongruent counterparts'' to describe objects like a right and left hand that are similar but non-superimposable.[98] The scientific concepts were formally solidified by Sir William Thomson (Lord Kelvin) in 1884, who coined the terms ''chiral'' and ''chirality'' (Greek words χειρ (cheir in Ancient Greek) meaning hand). He defined a chiral object as any geometrical figure whose mirror image cannot be brought to coincide with itself.[98] Later, Mislow refined the definition: ''an object is chiral and a chiroid if and only if it cannot be superposed on its mirror image by a proper congruence, otherwise it is achiral; two chiroids are heterochiral and enantiomorphs if and only if they are improperly congruent; and two chiroids are homochiral and homomorphs if and only if they are properly congruent.''

The concept of the tetrahedral carbon was published by van't Hoff (September 5, 1874) and Le Bel (November 5, 1874).[99]

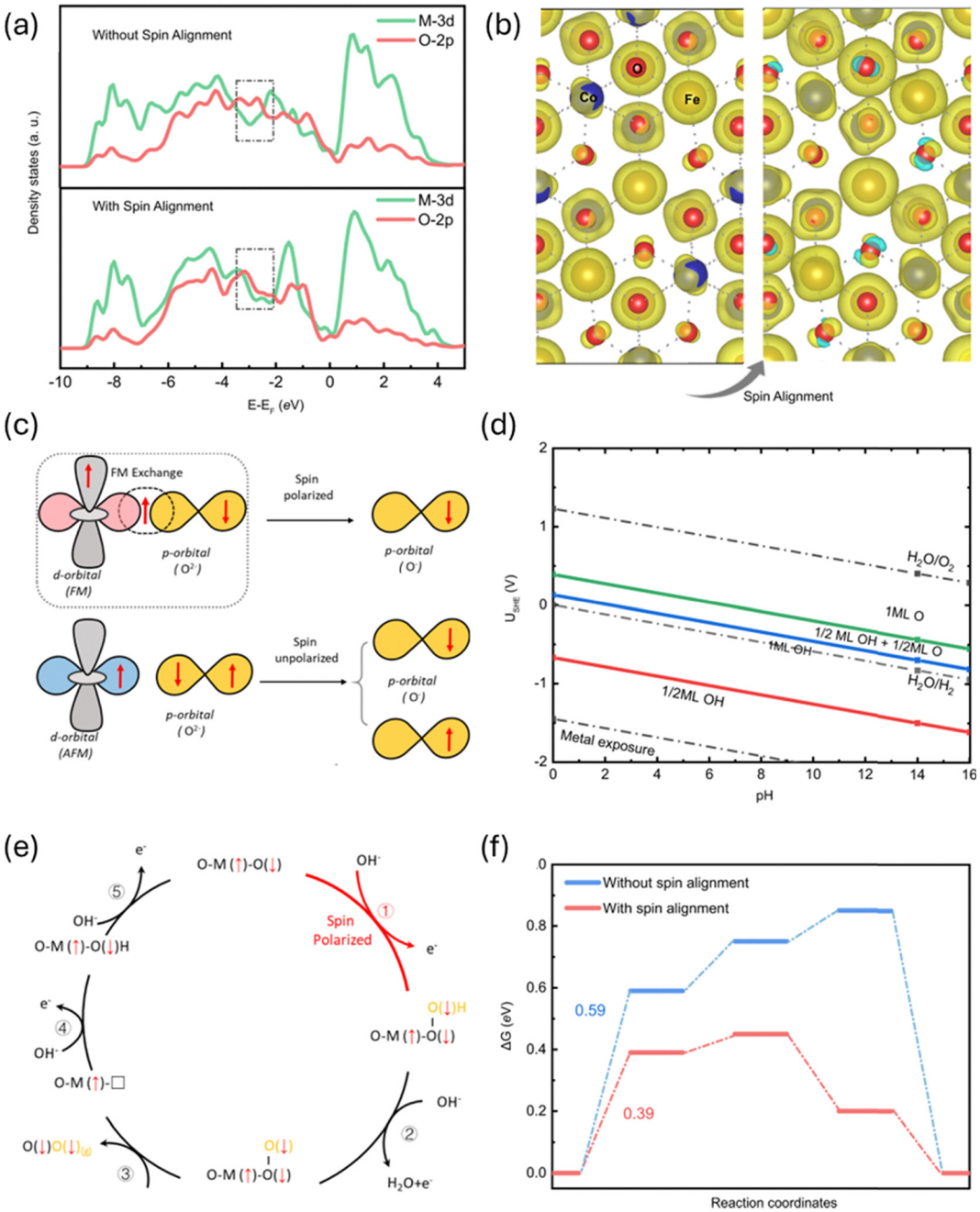

Fig. 9 Spin-polarized OER. (a) The projected density of states (PDOS) of $CoFe_2O_4$ without and with spin alignment. (b) The spin density for $CoFe_2O_4$ with and without spin alignment. (c) Schematic of the spin-exchange mechanism for OER. The first electron transfer step is promoted by spin polarisation through the FM exchange (QSEI), which gives smaller electronic repulsions and makes the adsorbed O species have a fixed spin direction. (d) The calculated Pourbaix diagram of the (111) surface of $CoFe_2O_4$. (e) The spin-polarisation mechanisms in OER starting from the step of O* + OH− → *OOH + e− step. (f) The free energy diagram of OER at 1.23 V (*vs.* RHE) with and without the spin alignment on the (111) surface of $CoFe_2O_4$ toward triplet oxygen production. Reproduced with permission.[89] Copyright Nature 2021.

Van't Hoff demonstrated that for a carbon atom bonded to four different univalent groups (which he termed "asymmetric"), the tetrahedral arrangement could produce "two and not more than two" spatial arrangements, which are mirror images of each other. While Le Bel argued that if a central atom was substituted with four different groups, creating an "asymmetric environment," the resulting molecule would be enantiomorphous with its reflection and exhibit optical activity. He concluded that this phenomenon compelled one to admit that the four groups must occupy the corners of a regular tetrahedron.

Geometric definitions

Chirality. All objects and their point groups can be classified as either chiral or achiral.[98] This classification is based on the presence or absence of improper rotations. An object is defined

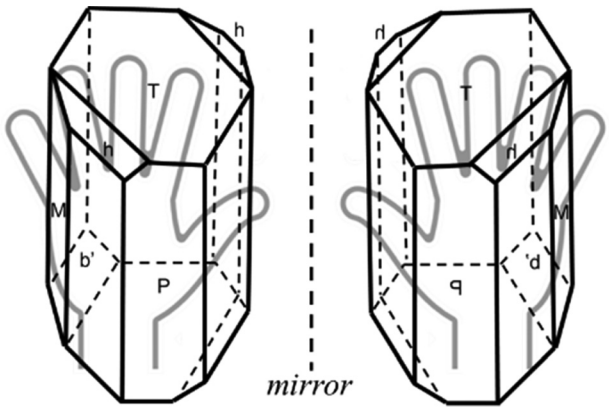

Fig. 10 Enantiomers of sodium ammonium tartrate showing left and right-handedness.

as chiral if its ''left-handed'' and ''right-handed'' mirror images are not superimposable; these non-superimposable pairs are known as enantiomers in chemistry. A chiral object lacks planes of symmetry and inversion centres, and its allowed symmetry elements are restricted to rotations, reflections, and translations. Chirality is a fundamental symmetry property that can be observed in elementary particles, molecules, and even macroscopic objects such as human hands.[100] Enantiomers cannot usually be distinguished by their basic physical properties because they share the same physical properties (mass, atomic composition, melting points, boiling points, density), and their chirality becomes apparent only when one chiral entity interacts with another. The interaction between chiral molecules depends on their stereochemical orientation. This stereochemical sensitivity is especially significant in biologically relevant applications such as drug and fragrance development and chemical biology.[100]

An object that lacks symmetry, particularly centrosymmetry (mirror planes or inversion centres) can be superimposed on its mirror image and is therefore achiral. These materials can be applied in a wide range of applications, including pyroelectricity, ferroelectricity, piezoelectricity, optical activity, and nonlinear optical behavior.[101]

The phenomenon of chirality generally occurs because a central atom is bonded to four different substituents in a three-dimensional orientation.[102] The current standard for defining and differentiating the absolute three-dimensional configuration of most chiral molecules is the Cahn–Ingold–Prelog (CIP) known as the R(rectus, or right) and S (sinister, or left) notation. The D/L notation is used for amino acids and sugars, with D (dextrorotatory) and L (laevorotatory) corresponding to the direction the molecule rotates polarized light. Today, the D/L notation is substituted by (+), which indicates clockwise rotation, and (−), which indicates counter-clockwise rotation.[102,103] For molecules that possess a distinct helical structure (like DNA or certain polymers), the R/S system is supplemented by the P (plus) and M (minus) designation to specify the screw sense. A screw displacement, also known as a rotation-translation,[98] is a motion of a compound that combines a simultaneous rotation and translation along the same axis (like screwing a bolt into place). When reporting a chiral compound, the sense of its optical rotation, which is experimentally measured (usually at the sodium D-line wavelength of 589 nm), is given separately in brackets, typically as (+) or (−).[103] The four substituent atoms attached to the chiral centre are assigned priorities based on their atomic number. The molecule is rotated from the atom with the highest priority (H1) to the lower priority (H3), while the lowest priority group (H4) is positioned behind the chiral center.[102] Priority is considered based on the substituent with the highest atomic number.

CISS mechanism

In the discussion around the nature of electron spin, it was noted that spin orbit coupling will deflect electrons of opposite spin in opposite directions, particularly for electrons bound to heavy nuclei. An analogous deflection occurs when electrons move through an asymmetric potential, such as where chirality has led to symmetry breaking. This has been named the chirality induced spin selectivity (CISS) effect. For electrons moving through chiral carbon structures, such as a DNA helix, the deflection suggests a spin–orbit coupling several orders of magnitude more significant than one would expect for the light carbon atoms in the structure.[104] The strength of the effect can be seen in the degree of electron polarisation or excess of polarised electrons that transit through the chiral structure. The degree of polarisation depends on the length of chiral environment through which the electron travels, and the time the electron spends in this environment: for a given chiral system, electrons with very high kinetic energy are less polarised, while those travelling through, for example, longer DNA strands are more polarised.[105,106]

The exact mechanism of this spin filtering has not yet become clear. Several possibilities, both classical and quantum, have been proposed. A classical electron moving through a chiral electric field sees a chiral magnetic field:

$$\vec{B} = -\frac{\vec{v} \times \vec{E}_{\text{chiral}}}{2c}$$

where v is the electron's velocity and c is the speed of light. The situation is similar to the Spin Hall effect discussed earlier, but now the geometry of the magnetic field adds an additional spatial discrimination.

At the same time, the broken symmetry may lead to the kind of backscattering suppression first described by Büttiker (1988).[107] The basic argument is that backscattered electrons must undergo a + π or − π phase shift, but these two possibilities interfere destructively, essentially eliminating backscattering for electrons of appropriate spin. This destructive interference reduces the likelihood all but the forward scattering paths. More of these electrons may propagate, leading to some spin polarisation.[104]

It is almost certain that the true mechanism requires electrons to interact with multiple chiral centres as they

Table 5 Comparison of chiral and achiral catalyst for electrocatalysis

Catalyst	Chirality	Tafel slope (mV dec^{-1}) OER	$\eta_{@10}$ (mV)	Tafel slope (mV dec^{-1}) ORR	$E_{1/2}$ (V)	Ref.
Co@CoO-L	Chiral	84.2	300	105	0.74	111
Co@CoO-DL	Achiral	92.4	350	107	0.70	
D-AgNWs@ composite	Chiral	115.5	—	—	0.74	112
L-AgNWs@ composite	Chiral	99.3	—	—	0.72	
AgNWs@ composite	Achiral	141.8	—	—	0.71	
Chiral-AgNWs@ composite	Chiral	—	—	—	0.74	
L-AgNWs	Chiral	—	—	—	0.69	
Achiral-AgNWs	Achiral	—	—	—	0.63	
L-SPNC-950-1	Chiral	—	—	106	0.87	119
L-Co-NiO	Chiral	100	350	—	—	120
DL-Co-NiO	Achiral	140	400	—	—	
D-Co-NiO	Chiral		380	—	—	
6%LS-CMMOFs/NF	Chiral	54	137	—	—	122
8%LS-CMMOFs/NF	Chiral	60	149	—	—	
4% LS-CM MOFs/NF	Chiral	79	156	—	—	
O-CMMOFs/NF	Chiral	91	182	—	—	
L-CuO	Chiral	93.5	308	—	—	123
D-Cuo	Chiral	105	308	—	—	
A-CuO	Achiral	117.1	Ca. 350	—	—	

propagate, as the introduction of even 1% of the opposite enantiomer has been found to supress the polarisation.[105]

An additional quantum effect that may both complement and complicate CISS engineering is coherence of electron pairs, particularly in ORR. The addition of classical electrons to an intermediate increases the electrostatic repulsion to additional electrons, raising activation energy of the multi-electron ORR process. However, if electron wave functions are appropriately correlated, this repulsion is significantly diminished, as found by Gupta *et al.*[108] Practically, this means that the various strategies to induce spin polarisation should take care to avoid decoherence of correlated electron pairs. For example, a chiral polymer layer will polarise electrons moving through it, with the spin excess increasing with layer thickness. However, a thicker layer also increases the chance for scattering events that will decohere electron pairs. A similar effect is seen for DNA strands of increasing length. Spin filters must therefore be designed to induce maximum spin excess while minimising the spatial extent and electrical resistance of the filter layer. Gupta *et al.* found that filters extending less than 7 nm in the direction of electron transport were optimal. This optimisation requirement may be the root cause for the variance in CISS enhancements reported in literature (Table 5), ranging from negligible to dramatic. Electrochemists must take care not to smother coherence and therefore conductivity in the pursuit of spin polarisation.

It will be in the interest of electrochemists to see which models emerge as accurate descriptions of the effect in the coming years: as following sections show, chiral spin selection is a powerful tool for enhancing the oxygen reactions, and an accurate model will aid rational catalyst design. For example, compact chiral polymers such as oligopeptides with a strong chiral electrical fields may be optimal, or the incorporation of heavier elements with large electron scattering cross sections may polarise currents more significantly.[105]

Whatever the details of the mechanism may be, the CISS effect influences the electron spin at the catalyst surface and so affects the reaction pathway. Activity and selectivity may be enhanced beyond the typical limitations defined by the volcano plot.[109]

Chiral functionalisation of electrocatalysts

Consequently, the last few decades have witnessed extensive research focused on the preparation of nanostructured chiral surfaces. Chirality can be introduced into achiral inorganic materials through the covalent functionalization of their surfaces with chiral organic molecules.[110] The most common technique involves covering the material with a highly ordered monolayer of a chiral molecule and, through covalent functionalization,[109,111,112] which involves chemically bonding chiral molecules to the surface. Introducing chirality into transition metal-based oxide catalysts through functionalization is a potent strategy for advancing ORR and OER efficiencies. Incorporating chirality into transition-metal oxides improves charge-transfer efficiency between oxygen species and the electrode by spin-polarizing the cathodic (ORR) and anodic (OER) currents through the CISS effect. In alkaline media, ORR can follow either a two-electron or a four-electron pathway, and in both cases, at least two electrons are required initially. ORR kinetics are inherently slow because oxygen can assume four possible spin-state configurations, with only one leading to product formation.[112]

Balo *et al.*[112] investigated how integrating chiral silver nanowires (AgNWs) can boost the electrocatalytic performance of an inverse spinel $CoFe_2O_4$ and reduced graphene oxide (rGO) composite. The use of silver was considered because of its ability to maintain its metallic state during ORR, its cost-effectiveness, and its ability to suppress the formation of H_2O_2 with metal loading over 20 wt% while completely reducing O_2.[113,114] The chiral AgNWs@composite showed

significantly improved ORR performance compared to the achiral version. It exhibited a ~68 mV positive shift in onset potential, nearly double the current density (5.3 *vs.* 2.7 mA cm^{-2}), and a higher half-wave potential (~0.74 *vs.* ~0.71 V). It also delivered greater mass activity (~5.5 *vs.* ~3.8 A g^{-1}) and higher kinetic current density at 0.74 V, confirming its enhanced catalytic efficiency. Both chiral and achiral AgNWs@composites followed a quasi-4-electron ORR pathway, indicating that chirality did not alter the reaction pathway. However, chirality improved the charge-transfer kinetics, as shown by the lower Tafel slope and reduced overpotential for the chiral composite. Integrating Ag nanowires with $CoFe_2O_4$–rGO enhances electronic conduction, increases surface area, and shortens diffusion paths, leading to better ORR activity than either pristine component alone. Similar improvements are observed for OER, with the chiral composite again delivering higher current density than the achiral version. The experimental results support the proposed mechanism in which chiral molecule-functionalized AgNWs combined with $CoFe_2O_4$–rGO enhance electrocatalytic activity through spin-selective charge transfer. The chiral catalyst polarizes electron spins, enabling more efficient interaction with triplet oxygen and accelerating ORR kinetics. Since ORR intermediates must adopt singlet spin states, achiral surfaces generate mixed-spin intermediates with higher activation barriers.[112] In contrast, the chiral composite provides spin-aligned electrons, lowering the barrier for forming singlet hydroxide intermediates and improving ORR selectivity. A similar spin-polarisation effect enhances OER, as hydroxide ions on the chiral surface release spin-polarized electrons that favour oxygen formation and reduce overpotential.

The study by Balo *et al.*,[112] also used chiral gold nanoparticles (AuNPs) to induce chirality onto a bimetallic spinel oxide ($MnCo_2O_4$). This created a catalyst where the AuNPs acted as electron spin filters through the CISS effect. The CISS effect, where the electron transport through a chiral molecule depends on the electron's spin and the molecule's handedness (enantiomeric form), provides a means to control the direction of the electron's spin relative to the molecular axis.[112] Electrons transmitted through this effect prefer a longitudinal spin orientation. The chiral AuNPs injected electrons that are spin-polarized. This specific spin alignment facilitates the spin-exchange effect when oxygen interacts with it, making the reaction pathway spin-allowed and significantly faster. This resulted in a higher current density of the chiral functionalized catalyst compared to that functionalized with an achiral AuNPs. Similarly, OER proceeded more efficiently on the chiral composite, shown by a significant reduction in the onset potential and overpotential. The onset potential for the OER was reduced by approximately 120 mV at 2.5 mA cm^{-2} current density when compared to the achiral composite catalyst. This is because hydroxide ions released electrons to the chiral electrode in a spin-selective manner, facilitating the generation of triplet oxygen. Molecular oxygen has a triplet ground state, and chiral gold nanoparticles can inject spin-polarized electrons whose spin direction is defined relative to the chiral molecular axis. Proper spin orientation at the chiral catalyst strengthens spin-exchange interactions, whereas this advantage is absent in catalysts functionalized with achiral gold nanoparticles. This spin-polarisation mechanism offers a novel method to enhance charge transfer by aligning the cathodic current (for ORR) and anodic current (for OER) with the necessary spin configuration, which is highly essential for applications in renewable energy technology (*e.g.*, fuel cells and metal–air batteries).

Similar findings are reported by Sang *et al.*[115] on gold films as well as gold and silver nanoparticles. All three systems showed improved onset potential when the metal surfaces were coated with a layer of chiral molecules. The CISS effect was emphasized by thicker chiral layers, while conductivity was reduced, proving the need for optimising layer thickness for both conductivity and polarisation. They find that the mechanism of enhancement is two-fold. The injection of electrons with parallel spins is energetically favourable, as discussed in all CISS-related literature. Their reasoning is unusual, however: they calculate that oxygen undergoes Zeeman splitting as it approaches the chiral surface, and the state where its unpaired electrons are both antiparallel to the spin excess on the catalyst surface is significantly stabilised. They also independently confirm the entropic component calculated by Gracia *et al.*:[9] ORR on a surface with a spin excess is both statistically more likely and does not lead to a decrease in entropy, as is the case for a surface without spin excess.

Vadakkayil *et al.*[116] demonstrated a scalable way for the preparation of chiral cobalt oxide nanoparticle electrocatalysts doped *via* iron ($Co_{(3-x)}Fe_xO_4$). The effect of the CISS is used to create spin polarisation reaction intermediates, in so doing helping the effectiveness for OER. When associated with comparable achiral cobalt oxide nanoparticles, the chiral ($Co_{(3-x)}$-Fe_xO_4 electrocatalyst enhances Faraday efficiency, cuts overpotential, and alters the rate-determining step for OER. Moreover, in OER electrocatalysis course, an external magnetic field with a ferromagnetic electrode can spin filter the electron current, which increased the current density approximately by 100 mA cm^{-2}.

Crystals of ZnO having graded chirality were produced by means of chiral methionine molecules as symmetry-breaking agents. Magnetic circular dichroism (CD) spectroscopy in addition magnetic permeability atomic force probe microscopy (AFM) prove that the chiral structure has a spin-filtering role in the photogenerated carrier migration then induces spin polarisation of the carriers. The spin-polarized carrier not only has an extended lifetime but also can intensify the creation rate of triplet O_2 and hinder the development of singlet byproduct H_2O_2 throughout this reaction process.[117]

The standard and most frequent type of self-assembled monolayers (SAMs) used in electrochemistry is those based on thiols. These compounds contain a sulphur–hydrogen (–SH) group that creates a very strong, permanent bond with metals such as gold, silver, and mercury. However, other SAM types are available for different surfaces: alkyl silanes are used for oxide materials like SiO_2; carboxylic acids bind strongly to specific oxides such as alumina; and amines and phosphonic

acids are effective for surface modification of indium tin oxide (ITO).[118] Yu *et al.*[119] used L- and D-tartaric acid as chiral templates, resulting in a self-assembled, ordered 3D porous structure of spiral-like polyhedra composed of nitrogen-doped carbon nanosheets. The resulting material has a conductive 3D network while preserving the advantages of 2D nanosheets. The optimized catalyst (L-SPNC-950-1) demonstrated excellent ORR performance, with a more positive onset potential and a half-wave potential comparable to commercial Pt/C. The material was further applied in an Al-air battery with good performance. Park *et al.*[120] fabricated cobalt-doped nickel oxide (Co-NiO) with a chiral, helically twisted nanoplate structure grown directly on Ni foam using a one-step hydrothermal method. Chirality was introduced by L- or D-proline, yielding L- and D-Co-NiO variants with distorted, twisted morphologies. Spin-dependent charge transport measurements using magnetic conductive-probe AFM showed strong spin selectivity, with L-Co-NiO exhibiting ~60% spin polarisation at 5 V. Co doping increased the proportion of Ni^{3+} species, indicating enhanced hole concentration and improved electronic properties. The chiral Co-NiO catalysts also demonstrated good durability, retaining ~90% of their OER current after 15 hours of continuous testing. When used as the air-cathode catalyst in a rechargeable Zn–air battery, the chiral Co-NiO enables a high open-circuit potential (1.57 V), a low charge–discharge voltage gap (0.71 V), and exceptionally stable operation for 960 h (40 days), attributed to the suppressed formation of reactive singlet oxygen ($^1O_2$).

Metal-organic frameworks (MOFs) are a promising class of electrocatalysts due to their large surface area, highly tuneable design, and adjustable pore structure.[121] Despite their potential, most conventional MOFs reported to date face several performance issues that limit their effectiveness as electrocatalysts: (a) poor mass permeability and electrical conductivity. (b) Low crystallinity, and the clogging of active metal sites by the surrounding organic ligands. Chiral Framework Materials (CMMOFs) are an emerging type of MOF that conveniently addresses these limitations, offering significant potential in catalysis due to the enhanced structure and porosity.[122] Lattice strain was effectively and controllably introduced into the CMMOFs by replacing a portion of the disulfonic acid linkers with mono-sulfonic acid linkers. The optimal strain level was found to be a 6% lattice expansion on nickel foam (6%LS-CMMOFs\NF), showing significantly improved performance for both the OER (η_{10} = 137 mV) and the hydrogen evolution reaction (HER, η_{10} = 100 mV) under alkaline conditions.

Further examples of chirality applied to OER/ORR electrocatalysis are shown in Table 5.

DFT - chirality

Li *et al.*[123] used DFT to understand how chirality affects copper oxide nanostructures during the OER. They created models of CuO surfaces in two ways: a normal, achiral form and a chiral form where nanosheets were stacked with a small helical twist to break mirror symmetry. Using spin-polarized DFT, they examined the electronic structure, band behaviour, and density of states (DOS). Their findings showed that chirality changes how electrons are distributed, leading to stronger spin splitting and higher spin polarisation than in normal CuO.

They also studied how key OER intermediates *OH, *O, and *OOH interact with both achiral and chiral CuO surfaces. The free-energy diagrams revealed that chiral CuO lowers the energy barriers, especially for forming the *OOH intermediate, which is usually the slowest step in OER. This reduction in energy makes the catalytic activity better, as also observed in experiments. The chirality-induced spin-polarized states couple more easily with oxygen species, helping O–O bond formation and speeding up the reaction.

They showed that the use of chirality is a promising way to improve spin-dependent catalytic processes in water splitting. Fig. 11 clearly demonstrates that chiral CuO reduces the energy needed to form *OOH compared to achiral CuO, helping charge transfer occur more easily and enhancing OER performance.

Characterization

At the atomic and molecular levels, chirality, manifested through asymmetric lattices or ligands, must be linked to macroscopic phenomena such as spin polarisation and electrocatalytic efficiency. *Operando* techniques must combine real-time data collections on the active material under real-world operating conditions in combination with electrochemical measurements. Often this is done using flow cells or modified three-electrode setups to capture transient species and spin dynamics. For chiral systems, these methods reveal how asymmetric environments induce spin filtering during electron transfer, enhancing OER/ORR efficiency beyond traditional scaling relations. Key strategies include the integration of external fields (magnetic or polarised light) to amplify CISS signals. The use of enantiopure *vs.* racemic controls to isolate chirality effects and multiscale probing: from atomic spin states to mesoscale helical structures. Recent reviews emphasise the need for standardised *operando* protocols to validate spin-dependent mechanisms.[37,124]

In chiral catalysts, XAS detects asymmetric coordination of *OH/*O intermediates, linking to CISS-enhanced kinetics. Recent examples show *operando* XAS applied to study enantiopure Fe–Ni oxides, revealing chiral intermediates participating in OER, with faster kinetics tied to optical activity.[40] Dual-channel XAS was applied to study spin regulation in OER. The measurements elucidated that spin polarisation enhances the kinetics of the oxygen evolution reaction (OER), a rate-limiting step that restricts the energy efficiency of water splitting.[125]

Operando Raman and infrared spectroscopies probe vibrational modes of surface species; surface-enhanced variants (SERS/SEIRAS) boost sensitivity. These techniques identify chiral ligand vibrations or asymmetric O–M bonds, linking to spin-selective adsorption. Recently, SEIRAS was applied to study chiral Fe–Ni oxides, confirming chiral intermediates in OER.[126]

Operando atomic force microscopy (AFM) and scanning tunnelling microscopy (STM) are applied for surface

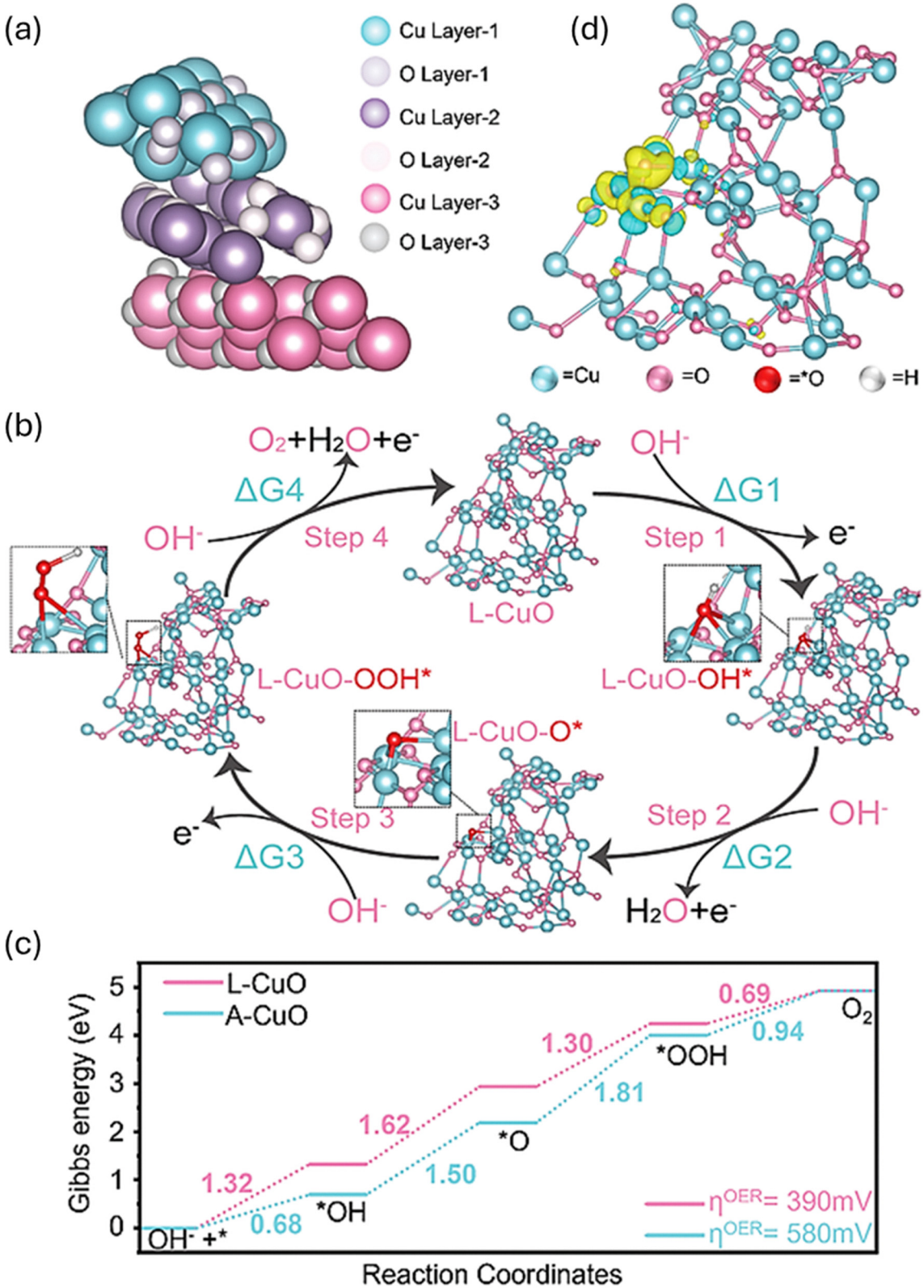

Fig. 11 DFT calculations. The optimized L-CuO model (a). Schematic illustration of different steps of OER over L-CuO, with optimum configurations of the key intermediates (b). The Gibbs free energy diagram of the key intermediates during OER on L-CuO and A-CuO at zero potential (c). Charge density difference of the L-CuO, where the yellow (cyan) iso-surface indicates charge accumulation (depletion) regions (d). Reproduced with permission.[123] Copyright Wiley 2024.

topography and current mapping. Here, spin-polarised currents are measured in real time, quantifying CISS efficiency. Recent advances cover in-liquid magnetic conductive-AFM (mc-AFM) for *operando* spin selectivity[7] as well as mc-AFM for spin blockade in chiral Au nanoparticles during OER.[106,127]

Operando microscopy and scanning probe techniques provide spatial resolution for visualising dynamic chirality and spin domains during reaction. Using bespoke cells, the methods enable the resolution of helical distortions or spin-polarised domains in chiral nanoparticles during reaction. Recently, Cryo-*operando* TEM was used, where chiral hydration in OER was preserved.[128] *Operando* STEM has been applied to chiral PdGa crystals for ORR, directly confirming spin polarisation.[129]

Morphological asymmetry

In this section we examine the synthesis and application of catalysts with explicitly chiral morphologies, as opposed to the more subtle chiral functionalisation or induction discussed thus far. The relationship between catalyst morphology and activity has long been an area of interest, as various shapes and heterostructures allow for unique active sites and charge transfer properties.[20] Asymmetry on this scale is simple to track through electron microscopy or small angle scattering experiments. New challenges arise however in degradation of delicate morphologies, and syntheses are challenging and may be resistant to scaling up.

Synthesis approach

The synthesis of asymmetric nanoparticles (ANPs) with defined chirality is a sophisticated art, moving away from thermodynamic equilibrium towards kinetically controlled growth. The methods generally used requires the application of an asymmetric influence to impart handedness to the structures.[130] Common strategies to establish this chiral bias involve the use of chiral directing agents, such as chiral ligands, templates or the application of magnetic fields, circularly polarized light, or macroscopic shear. These synthetic methods are primarily classified into two categories: structural engineering and surface engineering. The former constitutes a direct pathway, frequently utilizing chiral templates or physical deposition techniques. In contrast, surface engineering relies on an indirect mechanism where chirality is transferred from chiral molecular adsorbates to the achiral nanomaterial framework. Below is a brief overview of these methods and their influence on electrocatalytic performance.

Structural engineering

The chiral template-assisted methods offer a flexible and efficient pathways for synthesizing nanomaterials with complex hierarchical structures and enhanced functional properties.[131] Chiral templates can be categorized as either organic soft templates, such as chiral hydrogels,[132] liquid crystals,[133] and DNA-directed assembly,[134] or inorganic hard templates.[135]

Organic soft templates

Chiral hydrogels emerge as versatile soft templates for the synthesis of asymmetric nanoparticle (ANP). The synthesis method leverage the three-dimensional polymer networks to encapsulate and direct the nucleation of transition metal precursors into chiral architectures.[136–141] These hydrogels, often derived from biocompatible polymers like chitosan or alginate modified with chiral ligands, exhibit tuneable porosity and mechanical compliance, enabling precise control over nanoparticle dimensions typically ranging from 5–20 nm in width and 50–200 nm in length. Their hydrated environment fosters enantioselective metal deposition, as demonstrated in studies where hydrogel-confined Co and Ni clusters formed helical ANPs with enhanced spin polarisation for ORR, where overpotentials dropped by up to 50 mV compared to non-templated counterparts. Varying hydrogel cross-linking density and pH further modulates the chiral induction, yielding ANPs with adjustable plasmonic responses and catalytic selectivity, particularly in alkaline OER conditions.

In comparison, liquid crystal (LC) templating harnesses the self-organized anisotropic phases, such as cholesteric or smectic, to impose long-range helical order on ANPs, promoting uniform alignment and superior chiroptical properties. LCs, including those based on rod-like calamitic molecules or discotics, guide nanoparticle assembly at critical concentrations around 2–5 wt%, transitioning from isotropic dispersions to birefringent chiral nematic phases observable *via* polarized optical microscopy. Research demonstrated that lyotropic liquid crystal-templated platinum alloys form ordered nanoporous films with interconnected structures, enhancing electrocatalytic active area and charge transfer, resulting in improved ORR and OER performances. Entropic driving forces stabilize these ordered phases, enabling precise tuning of pitch length and surface anisotropy, which strengthen CISS effects and spin-polarized electron transfer. While hydrogels excel in biocompatibility and local chirality transfer, LCs provide sharper structural periodicity, higher-order domains, and ease of scalability, although they require tighter temperature control during synthesis.

Hard templates

Inorganic hard templates, such as helical mesoporous silica or zeolites derived from enantiopure precursors, provide rigid scaffolds with precise helical pores (pitch lengths 100–500 nm) to template the deposition of transition metal ANPs like CoFeNi or Pt alloys, ensuring high-fidelity chirality transfer upon template etching.[109] These templates enable thermal annealing up to 800 °C for enhanced crystallinity without chirality loss, yielding ANPs with pronounced circular dichroism (CD) (g-factors >0.01) and helical facets, as verified by TEM and magneto chiral dichroism, outperforming soft templates in structural durability.

The CISS effect in hard-templated ANPs amplifies ORR/OER performance *via* spin-selective electron transfer, with silica-templated Pt-Co helices achieving $>80\%$ spin polarisation to

favour triplet O_2 pathways, reducing ORR $E_{1/2}$ by 40 mV and OER η_{10} to $\sim$280 mV while suppressing peroxides.[142] This spin filtering lowers *OOH/*OH adsorption barriers on octahedral sites, boosting mass activity 2–3-fold and stability ($>$500 h), as CISS-enhanced spin–orbit coupling stabilizes active configurations in bifunctional metal–air catalysts.

Challenges and future perspectives

Despite the significant and growing interest in spin polarised catalysts, their scale up and mass use is yet to be demonstrated, and practical considerations will remain even as the theory becomes more robust. Very challenging syntheses, for example when enantiomeric purity greater than 99% is required, must be made cost effective. As always with catalysts, the stability of these systems will be an integral factor when it comes to their viability in technology. Spin polarisation is a low entropy state, and while this makes the oxygen reactions more thermodynamically favourable it also inevitably means that catalyst degradation will also be thermodynamically favourable. Degradation will take many forms, depending on the approach: magnetic order may decay, chirality may invert, and macroscopic asymmetry may be lost as morphology changes over time and use. These will be particularly evident in bifunctional applications, such as metal air battery cathodes, as different operating potentials lead to restructuring or complete phase changes.[143]

DFT

Despite significant progress in understanding spin effects in electrocatalysis, several challenges and opportunities remain. Future research should focus on coupling spin dynamics with reaction kinetics through advanced computational approaches such as time-dependent DFT and non-collinear magnetism. These methods can provide deeper insight into how spin states evolve during catalytic reactions and how they influence reaction rates and selectivity.

Another promising direction is the integration of magnetic field control into *operando* electrochemical cells, which would allow real-time observation and manipulation of spin-dependent processes under realistic reaction conditions. Such experiments could directly correlate spin polarisation with catalytic activity, providing valuable feedback for catalyst design.

In addition, combining machine learning with spin-polarized DFT offers a powerful strategy for accelerating catalyst discovery. By learning from existing datasets, machine learning models can predict spin-related properties and identify promising materials with optimal spin configurations for specific electrochemical reactions.

Finally, the emerging concept of ''spintronic electrocatalysts'' where magnetic and catalytic functionalities are coupled, opens new avenues for developing next-generation materials for sustainable energy conversion and storage devices. These systems could enable more efficient and selective reactions by controlling electron spin as an additional degree of freedom in catalysis.

Characterisation

While *operando* synchrotron methods like XAS and XMCD dominate, several novel techniques could be adapted for chiral electrocatalysts in OER/ORR to probe spin polarisation more directly or at higher resolutions; however, these techniques remain mostly underexplored or unapplied. A brief overview of these methods follows.

1. *Operando* neutron scattering (*e.g.*, neutron reflectometry or inelastic neutron scattering): neutrons are sensitive to magnetic moments and light elements (*e.g.*, H, O), making them ideal for studying spin dynamics and hydration layers in chiral interfaces during OER/ORR. This could reveal how chiral lattices induce spin alignment in water-splitting intermediates without the radiation damage issues of X-rays. Although applied to battery electrocatalysis, neutron scattering has not yet been used to study chiral spin effects. *Operando* neutron scattering enables time-resolved studies of structural and dynamic changes in electrochemical systems, including electrocatalysis for hydrogen production. The ability to conduct real-time, non-destructive probing of working devices under realistic conditions, linking atomic-scale reactions to mesoscale performance, makes neutron scattering an attractive technique. Neutrons' high sensitivity to light elements (H, O) allows for studying hydrogen/oxygen-involved dynamics in OER/ORR without interference from heavy metals. Enhancements to the second target station at ORNL's spallation source provide $\sim$100$\times$ increase in brightness, allowing time-resolved measurements (seconds or better), small-sample analysis, and broad spatiotemporal scales, improving kinetics resolution for irreversible electrochemical processes.[144] Multimodal integration is also possible, where neutrons are combined with X-ray, Raman, and conductivity measurements to provide quantitative mechanistic insights into interfacial evolution and degradation. However, some challenges need to be addressed, such as the need for standardised, neutron-compatible sample environments (*e.g.*, electrolysers with gas/D_2O feeds, optical access for photoexcitation, auto-sample changers) to enable *operando* multi-modal studies. Current setups require improvements in reliability, temperature stability, and alignment. Software bottlenecks for rapid data analysis in *operando* settings;[145] existing tools lag behind high-rate data collection at STS, requiring AI-assisted real-time steering and digital twins.

2. Ultrafast pump-probe spectroscopy, such as femtosecond X-ray or optical pump-probe: these techniques would allow the capture of transient spin states and electron dynamics in chiral catalysts on ps-fs timescales, elucidating CISS during fast OER/ORR steps like O–O bond formation.[146] Synchrotron or free-electron laser sources (*e.g.*, XFEL) enable this, but applications to spin-polarised electrocatalysis are still in their infancy; they could be extended to chiral systems to probe non-equilibrium spin flips under bias.

3. *Operando* muon spin spectroscopy (μSR): μSR probes local magnetic fields and spin relaxation with high sensitivity,

potentially detecting CISS-induced spin polarisation in chiral metal centres during ORR/OER.[40] The application of this technique remains underexplored in electrocatalysis but could complement XMCD by offering bulk penetration without requiring strong external fields.

4. *Operando* nuclear magnetic resonance (NMR) spectroscopy: another largely underexplored method for electrocatalysis, *operando* NMR could track chiral ligand dynamics and spin interactions in OER/ORR intermediates, especially in solution-phase chiral systems.[147] It provides chemical specificity for light nuclei, filling gaps in synchrotron methods for non-crystalline materials.

5. Spin-polarised scanning electron microscopy (spin-SEM) or *Operando* spin-polarised STM: these methods could visualise surface spin domains at the nanoscale during reaction, but *operando* versions for electrocatalysis are rare.[148] The application of these methods may provide insights into how chirality directs spin-selective electron pathways in OER/ORR, extending *ex situ* probes.

Roadmap

Looking ahead (Fig. 12), advancing spin-engineered OER and ORR electrocatalysis will require a coordinated research effort that integrates materials design, *operando* characterisation, theoretical development, and device-level validation. On the materials side, the field must move beyond empirical discovery toward predictive synthesis of catalysts with stable, well-defined spin polarisation under realistic operating conditions. In parallel, next-generation *operando* techniques-such as spin-resolved XAS/XMCD, neutron-based probes, spin-polarised scanning microscopies, and ultrafast magneto-optical spectroscopy-must be adapted to liquid electrochemical environments to directly track spin states and their evolution. Theoretical progress is equally crucial: non-collinear DFT, open-shell multireference methods, and spin-transport models need to be refined to capture dynamic spin transitions, electron–phonon coupling, and CISS-mediated charge transfer with greater accuracy. Machine learning and high-throughput computational screening will help identify new classes of spin-active materials, but only if coupled with experimentally validated spin descriptors and realistic reaction environments. Finally, translating spin-based catalytic enhancements into practical technologies will require systematic evaluation of field-assisted devices, chiral–inorganic hybrid electrodes, and magnetically ordered catalysts in full-cell configurations like zinc–air and electrolyser system to quantify durability, scalability, and energy efficiency gains.

On the journey to practical applications, there are opportunities to study longevity, scalability, and cost optimisation of such systems. In addition, the challenge of incorporating

Fig. 12 Roadmap to practical spin-controlled electrocatalysts.

powerful magnetic fields into energy systems may be an opportunity for innovation in the realm of magnetic field shielding, shaping and projection.[149,150]

By aligning advances across these domains, the field can progress from compelling proof-of-concept demonstrations to a robust, mechanistically grounded framework for designing next-generation spintronic electrocatalysts.

Conclusion

The past decade has witnessed the emergence of spin as a powerful, previously underappreciated dimension in the design of oxygen electrocatalysts. While the conventional descriptors of occupancy, d-band centre, charge-transfer energy, and p–d hybridisation continue to guide rational catalyst optimisation, they are fundamentally limited by well-established scaling relationships. The incorporation of spin control introduces an additional quantum degree of freedom. Because water is singlet and key intermediates (*OH, *O, and *OOH) exist in distinct spin states, and because O_2 itself is a triplet species, the alignment between catalyst spin configuration and intermediate spin multiplicity governs both thermodynamics and electron-transfer kinetics. This review has shown that controlling catalyst spin states offers a path to modulate reaction barriers in ways inaccessible to classical catalyst design.

It is clear that catalysts that maintain well-defined, spin-polarised electronic structures during operation facilitate more efficient coupling between the spin states of electrons, surface intermediates, and products. High-spin transition metal centres in oxides and (oxy)hydroxides often show improved OER/ORR activity due to enhanced exchange interactions, while strained lattices or heteroatom dopants can stabilise favourable spin configurations. Magnetic-field-assisted catalysis adds further tunability, coupling ferromagnetic exchange with mass-transfer benefits under certain conditions. Meanwhile, the CISS effect has opened an entirely new class of spintronic electrocatalysts, where electron transmission through asymmetric organic or inorganic motifs produces spin-filtered currents that break traditional volcano-type limitations. The synergy between structural asymmetry, spin filtering, and surface chemistry is becoming increasingly clear, while the need for efficient electron conduction through these surface features demands careful optimisation.

Despite this progress, significant challenges remain. Spin-polarised states are inherently low-entropy and can decay rapidly under electrochemical conditions, particularly in materials prone to reconstruction or ligand loss. Chiral or asymmetrically structured catalysts may suffer from morphological degradation, while catalysts relying on external magnetic fields may face scalability concerns. The mechanistic underpinnings of CISS remain contested, necessitating deeper theoretical and experimental scrutiny. Furthermore, the field currently lacks standardised *operando* protocols capable of quantifying spin polarisation, distinguishing between electronic and mass-transport contributions, and linking transient spin dynamics to catalytic turnover.

Opportunities for future development are abundant. Advanced computational methods including non-collinear DFT, time-dependent magnetisation dynamics, and machine-learning-accelerated spin screening will be essential for identifying materials with optimal spin characteristics. On the experimental side, integration of magnetic-field control into *operando* cells, *operando* neutron scattering, spin-resolved STM/AFM, and emerging spin-sensitive spectroscopy techniques promises to unravel the complex interplay between spin, structure, and reactivity.

Ultimately, the convergence of materials science, chiral chemistry, and electrocatalysis suggests a future in which spintronic electrocatalysts form a foundational pillar of renewable energy technologies, enabling water electrolysers, fuel cells, and metal–air batteries that surpass the efficiency ceilings imposed by conventional catalyst design.

Author contributions

Ernst H. Hechter - conceptualisation, project administration, original draft writing, review and editing. Augustus K. Lebechi - project administration, original draft writing, review and editing. Desalegn N. Gemechu - conceptualisation, original draft writing. Fitsum A. Hailu - original draft writing. Lesego Gaolathe - original draft writing, review and editing. Dean H. Barrett - Supervision, conceptualisation, original draft writing, review and editing. Thapelo P. Mofokeng - original draft writing, review and editing. Kenneth I. Ozoemena - conceptualisation, supervision, review and editing.

Conflicts of interest

There are no conflicts to declare.

Data availability

No primary research results, software or code have been included and no new data were generated or analysed as part of this review.

Acknowledgements

The authors are grateful for the support of the DSTI/NRF/Wits SARChI Chair on Materials Electrochemistry and Energy Technologies (MEET) (UID #132739).

References

1 X. Zhao, Z. Hao, X. Zhang, L. Li, Y. Gao and L. Liu, Alkaline Oxygen Reduction/Evolution Reaction Electrocatalysis: A Critical Review Focus on Orbital Structure, Non-Noble Metal Catalysts, and Descriptors, *Chem. Eng. J.*, 2024, **497**, 155005, DOI: 10.1016/j.cej.2024.155005.
2 Z. Feng, C. Dai, P. Shi, X. Lei, R. Guo, B. Wang, X. Liu and J. You, Seven Mechanisms of Oxygen Evolution Reaction Proposed Recently: A Mini Review, *Chem. Eng. J.*, 2024, **485**, 149992, DOI: 10.1016/j.cej.2024.149992.

3 E. Fabbri and T. J. Schmidt, Oxygen Evolution Reaction—The Enigma in Water Electrolysis, *ACS Catal.*, 2018, **8**(10), 9765–9774, DOI: 10.1021/acscatal.8b02712.
4 H. Li, Q. Quan, C. Wong and J. C. Ho, Spin-Selective Catalysts for Oxygen-Involved Electrocatalysis, *Adv. Energy Sustainability Res.*, 2025, **6**(5), 2400326, DOI: 10.1002/aesr.202400326.
5 J. Li, Oxygen Evolution Reaction in Energy Conversion and Storage: Design Strategies Under and Beyond the Energy Scaling Relationship, *Nano-Micro Lett.*, 2022, **14**(1), 112, DOI: 10.1007/s40820-022-00857-x.
6 J. Wang, C.-X. Zhao, J.-N. Liu, D. Ren, B.-Q. Li, J.-Q. Huang and Q. Zhang, Quantitative Kinetic Analysis on Oxygen Reduction Reaction: A Perspective, *Nano Mater. Sci.*, 2021, **3**(3), 313–318, DOI: 10.1016/j.nanoms.2021.03.006.
7 E. Van Der Minne, P. Vensaus, V. Ratovskii, S. Hariharan, J. Behrends, C. Franchini, J. Fransson, S. S. Dhesi, F. Gunkel, F. Gossing, G. Katsoukis, U. I. Kramm, M. Lingenfelder, Q. Lan, Y. V. Kolen'ko, Y. Li, R. R. Mohan, J. McCord, L. Ni, E. Pavarini, R. Pentcheva, D. H. Waldeck, M. Verhage, A. Yu, Z. J. Xu, P. Torelli, S. Mauri, N. Avarvari, A. Bieberle-Hütter and C. Baeumer, Spin Matters: A Multidisciplinary Roadmap to Understanding Spin Effects in Oxygen Evolution Reaction During Water Electrolysis, *Adv. Energy Mater.*, 2025, e03556, DOI: 10.1002/aenm.202503556.
8 L. Lin, P. Su, Y. Han, Y. Xu, Q. Ni, X. Zhang, P. Xiong, Z. Sun, G. Sun and X. Chen, Advances in Regulating the Electron Spin Effect toward Electrocatalysis Applications, *eScience*, 2025, **5**(1), 100264, DOI: 10.1016/j.esci.2024.100264.
9 J. Gracia, J. Munarriz, V. Polo, R. Sharpe, Y. Jiao, J. W. Niemantsverdriet and T. Lim, Analysis of the Magnetic Entropy in Oxygen Reduction Reactions Catalysed by Manganite Perovskites, *ChemCatChem*, 2017, **9**(17), 3358–3363, DOI: 10.1002/cctc.201700302.
10 Z. Chen, X. Li, H. Ma, Y. Zhang, J. Peng, T. Ma, Z. Cheng, J. Gracia, Y. Sun and Z. J. Xu, Spin-Dependent Electrocatalysis, *Natl. Sci. Rev.*, 2024, **11**(9), nwae314, DOI: 10.1093/nsr/nwae314.
11 S. Chen, Y. Chen, Y. Zhao, L. Zhang, C. Zhu, Y. Zhang, S. Liu, S. Xia, J. Yu, B. Ding and J. Yan, Status and Strategies for Fabricating Flexible Oxide Ceramic Micro-Nanofiber Materials, *Mater. Today*, 2022, **61**, 139–168, DOI: 10.1016/j.mattod.2022.11.004.
12 Y. Yang, Y. Li, B. Yin and C. Zhang, The Design of Spin Catalysts: Breakthroughs toward Efficient Energy Conversion, *ChemElectroChem*, 2025, **12**(14), e202500023, DOI: 10.1002/celc.202500023.
13 M. Weller; T. Overton; J. Rourke and F. Armstrong, *Inorganic Chemistry*, OUP, Oxford, 2014.
14 S. Huo, X. Wang, Y. Chen, H. Yue, L. Li and J. Zou, Spin Effects in Electrocatalysis: Mechanisms, Catalyst Engineering, Modulation, and Applications, *Mater. Sci. Eng., R*, 2025, **164**, 100967, DOI: 10.1016/j.mser.2025.100967.
15 P. Atkins, J. De Paula and J. Keeler, *Atkins' physical chemistry*, Oxford University Press, 11th edn, 2017.
16 M. Blume and R. E. Watson, Theory of Spin-Orbit Coupling in Atoms. I. Derivation of the Spin-Orbit Coupling Constant, *Proc. R. Soc. London, Ser. A*, 1962, **270**(1340), 127–143.
17 V.-H. Do and J.-M. Lee, Orbital Occupancy and Spin Polarization: From Mechanistic Study to Rational Design of Transition Metal-Based Electrocatalysts toward Energy Applications, *ACS Nano*, 2022, **16**(11), 17847–17890, DOI: 10.1021/acsnano.2c08919.
18 Q. Liang, G. Brocks and A. Bieberle-Hütter, Oxygen Evolution Reaction (OER) Mechanism under Alkaline and Acidic Conditions, *J. Phys. Energy*, 2021, **3**(2), 026001, DOI: 10.1088/2515-7655/abdc85.
19 X. Li, Z. Cheng and X. Wang, Understanding the Mechanism of the Oxygen Evolution Reaction with Consideration of Spin, *Electrochem. Energy Rev.*, 2021, **4**(1), 136–145, DOI: 10.1007/s41918-020-00084-1.
20 J. Han, J. Sun, S. Chen, S. Zhang, L. Qi, A. Husile and J. Guan, Structure–Activity Relationships in Oxygen Electrocatalysis, *Adv. Mater.*, 2024, **36**(47), 2408139, DOI: 10.1002/adma.202408139.
21 X. Ren, T. Wu, Y. Sun, Y. Li, G. Xian, X. Liu, C. Shen, J. Gracia, H.-J. Gao, H. Yang and Z. J. Xu, Spin-Polarized Oxygen Evolution Reaction under Magnetic Field, *Nat. Commun.*, 2021, **12**(1), 2608, DOI: 10.1038/s41467-021-22865-y.
22 L. Tan, X. Wu, H. Wang, J. Zeng, B. Mei, X. Pan, W. Hu, M. Faiza, Q. Xiao, Y. Zhao, C. Fu, C. Lin, X. Li and W. Luo, Ferromagnetic-Interaction-Induced Spin Symmetry Broken in Ruthenium Oxide for Enhanced Acidic Water Oxidation, *ACS Catal.*, 2024, **14**(15), 11273–11285, DOI: 10.1021/acscatal.4c02736.
23 L. Li, J. Zhou, X. Wang, J. Gracia, M. Valvidares, J. Ke, M. Fang, C. Shen, J.-M. Chen, Y.-C. Chang, C.-W. Pao, S.-Y. Hsu, J.-F. Lee, A. Ruotolo, Y. Chin, Z. Hu, X. Huang and Q. Shao, Spin-Polarization Strategy for Enhanced Acidic Oxygen Evolution Activity, *Adv. Mater.*, 2023, **35**(35), 2302966, DOI: 10.1002/adma.202302966.
24 T. Sun, Z. Tang, W. Zang, Z. Li, J. Li, Z. Li, L. Cao, J. S. Dominic Rodriguez, C. O. M. Mariano, H. Xu, P. Lyu, X. Hai, H. Lin, X. Sheng, J. Shi, Y. Zheng, Y.-R. Lu, Q. He, J. Chen, K. S. Novoselov, C.-H. Chuang, S. Xi, X. Luo and J. Lu, Ferromagnetic Single-Atom Spin Catalyst for Boosting Water Splitting, *Nat. Nanotechnol.*, 2023, **18**(7), 763–771, DOI: 10.1038/s41565-023-01407-1.
25 W. H. Lee, M. H. Han, Y.-J. Ko, B. K. Min, K. H. Chae and H.-S. Oh, Electrode Reconstruction Strategy for Oxygen Evolution Reaction: Maintaining Fe-CoOOH Phase with Intermediate-Spin State during Electrolysis, *Nat. Commun.*, 2022, **13**(1), 605, DOI: 10.1038/s41467-022-28260-5.
26 M. Li, X. Wang, K. Liu, Z. Zhu, H. Guo, M. Li, H. Du, D. Sun, H. Li, K. Huang, Y. Tang and G. Fu, Ce-Induced Differentiated Regulation of Co Sites via Gradient Orbital Coupling for Bifunctional Water-Splitting Reactions, *Adv. Energy Mater.*, 2023, **13**(30), 2301162, DOI: 10.1002/aenm.202301162.
27 J. Zhang, Y. Zhao, W. Zhao, J. Wang, Y. Hu, C. Huang, X. Zou, Y. Liu, D. Zhang, X. Lu, H. Fan and Y. Hou, Improving Electrocatalytic Oxygen Evolution through Local Field Distortion in Mg/Fe Dual-Site Catalysts, *Angew. Chem., Int. Ed.*, 2023, **62**(52), e202314303, DOI: 10.1002/anie.202314303.
28 Y. Wang, Y. Shang, Z. Cao, K. Zeng, Y. Xie, J. Li, Y. Yao and W. Gan, Highly Efficient, Field-Assisted Water Splitting Enabled by a Bifunctional Ni3Fe Magnetized Wood Carbon, *Chem. Eng. J.*, 2022, **439**, 135722, DOI: 10.1016/j.cej.2022.135722.
29 J. Chen, Y. Ling, X. Yu, G. Wang, L. Huang, A. He, Q. Fan, S. Qin, S. Xiang, M. Xu, Z. Han, J. Du and Q. Xu, Water Oxidation on CrMnFeCoNi High Entropy Alloy: Improvement through Rejuvenation and Spin Polarization, *J. Alloys Compd.*, 2022, **929**, 167344, DOI: 10.1016/j.jallcom.2022.167344.
30 P. Guo, Y. Zhang, F. Han, Y. Du, B. Song, W. Wang, X. Wang, Y. Zhou and P. Xu, Unveiling the Coercivity-Induced Electrocatalytic Oxygen Evolution Activity of Single-Domain $CoFe_2O_4$ Nanocrystals under a Magnetic Field, *J. Phys. Chem. Lett.*, 2022, **13**(32), 7476–7482, DOI: 10.1021/acs.jpclett.2c01843.
31 Y. Wang, P. Meng, Z. Yang, M. Jiang, J. Yang, H. Li, J. Zhang, B. Sun and C. Fu, Regulation of Atomic Fe-Spin State by Crystal Field and Magnetic Field for Enhanced Oxygen Electrocatalysis in Rechargeable Zinc-Air Batteries, *Angew. Chem., Int. Ed.*, 2023, **62**(28), e202304229, DOI: 10.1002/anie.202304229.
32 Y. Su, X. Ding and J. Yuan, Trimetallic Nanoarchitectonics of FeCoNi Catalyst with Modulated Spin Polarization for Enhanced Oxygen Reduction Performance, *Int. J. Hydrogen Energy*, 2024, **55**, 893–903, DOI: 10.1016/j.ijhydene.2023.11.248.
33 C. Chen, Y. Li, A. Huang, X. Liu, J. Li, Y. Zhang, Z. Chen, Z. Zhuang, Y. Wu, W.-C. Cheong, X. Tan, K. Sun, Z. Xu, D. Liu, Z. Wang, K. Zhou and C. Chen, Engineering Molecular Heterostructured Catalyst for Oxygen Reduction Reaction, *J. Am. Chem. Soc.*, 2023, **145**(39), 21273–21283, DOI: 10.1021/jacs.3c05371.
34 T. Tang, Y. Wang, J. Han, Q. Zhang, X. Bai, X. Niu, Z. Wang and J. Guan, Dual-Atom Co-Fe Catalysts for Oxygen Reduction Reaction, *Chin. J. Catal.*, 2023, **46**, 48–55, DOI: 10.1016/S1872-2067(22)64189-5.
35 Q. Xue, Y. Wang, M. Jiang, R. Cheng, K. Li, T. Zhao and C. Fu, Engineering Electronic Spin State of a CoNi Alloy for an Efficient Oxygen Reduction Reaction, *ACS Appl. Energy Mater.*, 2023, **6**(3), 1888–1896, DOI: 10.1021/acsaem.2c03831.
36 X. Liao, R. Lu, L. Xia, Q. Liu, H. Wang, K. Zhao, Z. Wang and Y. Zhao, Density Functional Theory for Electrocatalysis, *Energy Environ. Mater.*, 2022, **5**(1), 157–185, DOI: 10.1002/eem2.12204.
37 Q. Zhou and J. Chen, Meticulous Design of Chiral Molecules in Efficient and Stable Perovskite Solar Cells, *Adv. Funct. Mater.*, 2025, **35**(38), 2502139, DOI: 10.1002/adfm.202502139.
38 Z. Xue, B. Wu, Z. Zhang, C. Lin, X. Li, Q. Zhang and K. Tao, Spin Selectivity Induced by the Interface Effect for Boosted Water

Oxidation, *ACS Catal.*, 2024, **14**(8), 5685–5695, DOI: 10.1021/acscatal.4c00142.
39 R. Kawondera, M. Bonechi, I. Maccioni, W. Giurlani, T. Salzillo, E. Venuti, D. Mishra, C. Fontanesi, M. Innocenti, G. Mehlana and W. Mtangi, Chiral ''Doped'' MOFs: An Electrochemical and Theoretical Integrated Study, *Front. Chem.*, 2023, 11, DOI: 10.3389/fchem.2023.1215619.
40 F. A. Garcés-Pineda, J. Yu, C. A. Mesa, S. Plana-Ruiz, D. Ruano, Y. Liang, M. Lingenfelder, S. Giménez and J. R. Galán-Mascarós, *Operando* Evidence on the Chirality-Enhanced Oxygen Evolution Reaction in Intrinsically Chiral Electrocatalysts, *Chem. Sci.*, 2025, **16**(13), 5475–5482, DOI: 10.1039/d4sc07927b.
41 Z. Fang, W. Zhao, T. Shen, D. Qiu, Y. Lv, X. Hou and Y. Hou, Spin-Modulated Oxygen Electrocatalysis, *Precis. Chem.*, 2023, **1**(7), 395–417, DOI: 10.1021/prechem.3c00059.
42 T. Lim, J. W. Niemantsverdriet and J. Gracia, Layered Antiferromagnetic Ordering in the Most Active Perovskite Catalysts for the Oxygen Evolution Reaction, *ChemCatChem*, 2016, **8**(18), 2968–2974, DOI: 10.1002/cctc.201600611.
43 J. Gracia, R. Sharpe and J. Munarriz, Principles Determining the Activity of Magnetic Oxides for Electron Transfer Reactions, *J. Catal.*, 2018, **361**, 331–338, DOI: 10.1016/j.jcat.2018.03.012.
44 R. Sharpe, T. Lim, Y. Jiao, J. W. (Hans) Niemantsverdriet and J. Gracia, Oxygen Evolution Reaction on Perovskite Electrocatalysts with Localized Spins and Orbital Rotation Symmetry, *ChemCatChem*, 2016, **8**(24), 3762–3768, DOI: 10.1002/cctc.201600835.
45 A. L. Buchachenko, L. V. Ruban, E. N. Step and N. J. Turro, Spin Catalysis of the Radical Recombination Reaction, *Chem. Phys. Lett.*, 1995, **233**(3), 315–318, DOI: 10.1016/0009-2614(94)01429-Y.
46 X. Xu and J. Guan, Spin Effect in Dual-Atom Catalysts for Electrocatalysis, *Chem. Sci.*, 2024, **15**(36), 14585–14607, DOI: 10.1039/D4SC04370G.
47 Y. Zhang, Q. Wu, J. Z. Y. Seow, Y. Jia, X. Ren and Z. J. Xu, Spin States of Metal Centers in Electrocatalysis, *Chem. Soc. Rev.*, 2024, **53**(16), 8123–8136, DOI: 10.1039/D3CS00913K.
48 M. A. Halcrow, Manipulating Metal Spin States for Biomimetic, Catalytic and Molecular Materials Chemistry, *Dalton Trans.*, 2020, **49**(44), 15560–15567, DOI: 10.1039/D0DT01919D.
49 S. Liu, B. Zhang, Y. Cao, H. Wang, Y. Zhang, S. Zhang, Y. Li, H. Gong, S. Liu, Z. Yang and J. Sun, Understanding the Effect of Nickel Doping in Cobalt Spinel Oxides on Regulating Spin State to Promote the Performance of the Oxygen Reduction Reaction and Zinc–Air Batteries, *ACS Energy Lett.*, 2023, **8**(1), 159–168, DOI: 10.1021/acsenergylett.2c02457.
50 L. Yang, R. He, M. Botifoll, Y. Zhang, Y. Ding, C. Di, C. He, Y. Xu, L. Balcells, J. Arbiol, Y. Zhou and A. Cabot, Enhanced Oxygen Evolution and Zinc-Air Battery Performance via Electronic Spin Modulation in Heterostructured Catalysts, *Adv. Mater.*, 2024, **36**(31), 2400572, DOI: 10.1002/adma.202400572.
51 R. R. Fernandes and A. Y. Tamijani, Design Optimization of Lattice Structures with Stress Constraints, *Mater. Des.*, 2021, **210**, 110026, DOI: 10.1016/j.matdes.2021.110026.
52 Y. Zhao, Z. Gao, N. C.-R. Chen, Y. Asakura, H. N. Nam, Q. M. Phung, Y. Kang, M. H. M. Leung, D. Jiang, L. Fu, L. Huang, T. Asahi and Y. Yamauchi, Ultrathin Mesoporous Metal-Organic Framework Nanosheets, *Adv. Mater.*, 2025, **37**(36), 2508105, DOI: 10.1002/adma.202508105.
53 C. Wang, Z. Wang, S. Mao, Z. Chen and Y. Wang, Coordination Environment of Active Sites and Their Effect on Catalytic Performance of Heterogeneous Catalysts, *Chin. J. Catal.*, 2022, **43**(4), 928–955, DOI: 10.1016/S1872-2067(21)63924-4.
54 F. Li, H. Ai, D. Liu, K. H. Lo and H. Pan, An Enhanced Oxygen Evolution Reaction on 2D CoOOH via Strain Engineering: An Insightful View from Spin State Transition, *J. Mater. Chem. A*, 2021, **9**(33), 17749–17759, DOI: 10.1039/D1TA03412J.
55 L. Wang, J. Liu, M. Wu, H. Wu, K. Li, Y. Shao, Z. Li and W. Wang, Strain-Induced Modulation of Spin Configuration in LaCoO3, *Front. Mater.*, 2020, **7**, 60, DOI: 10.3389/fmats.2020.00060.
56 T. Hou, R. Yang, J. Xu, X. He, H. Yang, P. W. Menezes and Z. Chen, In Situ Evolution of Bulk-Active γ-CoOOH with Immobilized Gd Dopants Enabling Efficient Oxygen Evolution Electrocatalysis, *Nanoscale*, 2024, **16**(33), 15629–15639, DOI: 10.1039/D4NR01743A.
57 Y. Luo and Y. Wu, Defect Engineering of Nanomaterials for Catalysis, *Nanomaterials*, 2023, **13**(6), 1116, DOI: 10.3390/nano13061116.
58 Z. Lu, W. Zhou, P. Huo, Y. Luo, M. He, J. Pan, C. Li and Y. Yan, Performance of a Novel TiO2 Photocatalyst Based on the Magnetic Floating Fly-Ash Cenospheres for the Purpose of Treating Waste by Waste, *Chem. Eng. J.*, 2013, **225**, 34–42, DOI: 10.1016/j.cej.2013.03.077.
59 X. Cheng, D. Wu, H. Xu and W. Zhang, Role of Heteroatom Doping in Enhancing the Catalytic Activities and Stability of Atomically Dispersed Metal Catalysts for Oxygen Evolution Reaction, *J. Phys. Chem. C*, 2024, **128**(29), 12101–12108, DOI: 10.1021/acs.jpcc.4c02747.
60 Z. Fang, M. Chai, Y. Lv, W. Zhao, X. Hou and Y. Hou, Origin of Spin-State Precise Modulation for Enhanced Oxygen Evolution Activity: Effect of Secondary Coordination Sphere, *Adv. Funct. Mater.*, 2024, **34**(22), 2315039, DOI: 10.1002/adfm.202315039.
61 Z.-D. He, R. Tesch, M. J. Eslamibidgoli, M. H. Eikerling and P. M. Kowalski, Low-Spin State of Fe in Fe-Doped NiOOH Electrocatalysts, *Nat. Commun.*, 2023, **14**(1), 3498, DOI: 10.1038/s41467-023-38978-5.
62 W. Wan, Y. Zhao, S. Wei, C. A. Triana, J. Li, A. Arcifa, C. S. Allen, R. Cao and G. R. Patzke, Mechanistic Insight into the Active Centers of Single/Dual-Atom Ni/Fe-Based Oxygen Electrocatalysts, *Nat. Commun.*, 2021, **12**(1), 5589, DOI: 10.1038/s41467-021-25811-0.
63 F. Liu, C. Shi, L. Pan, Z.-F. Huang, X. Zhang and J.-J. Zou, Manipulating the Spin State to Activate the Atomically Dispersed Fe–N–C Catalyst for Oxygen Reduction, *EES Catal.*, 2023, **1**(4), 562–570, DOI: 10.1039/D3EY00066D.
64 Y. Li, T. Wang, M. Asim, L. Pan, R. Zhang, Z.-F. Huang, Z. Chen, C. Shi, X. Zhang and J.-J. Zou, Manipulating Spin Polarization of Defected Co3O4 for Highly Efficient Electrocatalysis, *Trans. Tianjin Univ.*, 2022, **28**(3), 163–173, DOI: 10.1007/s12209-022-00320-3.
65 A. Métioui, Brief Historical Review about Magnetism: From the Ancient Greeks up the Beginning of the XXth Century, *J. Biomed. Res. Environ. Sci.*, 2022, **3**, DOI: 10.37871/jbres1561.
66 Y. Wang, Y. Zhang, S. Xia, J. Yu and B. Ding, Direct Magnetic Reinforcement of Electrocatalytic ORR/OER with Electromagnetic Induction of Magnetic Catalysts, *Adv. Mater.*, 2021, **33**, 2007525, DOI: 10.1002/adma.202007525.
67 A. Yu, Y. Zhang, S. Zhu, T. Wu and Z. J. Xu, Spin-Related and Non-Spin-Related Effects of Magnetic Fields on Water Oxidation, *Nat. Energy*, 2025, **10**(4), 435–447, DOI: 10.1038/s41560-025-01744-6.
68 J. Li, J. Ma, Z. Ma, E. Zhao, K. Du, J. Guo and T. Ling, Spin Effect on Oxygen Electrocatalysis, *Adv. Energy Sustainability Res.*, 2021, **2**(8), 2100034, DOI: 10.1002/aesr.202100034.
69 J. Qian, T. Wang, Z. Zhang, Y. Liu, J. Li and D. Gao, Engineered Spin State in Ce Doped LaCoO3 with Enhanced Electrocatalytic Activity for Rechargeable Zn-Air Batteries, *Nano Energy*, 2020, **74**, 104948, DOI: 10.1016/j.nanoen.2020.104948.
70 J.-Y. Zhang, Y. Yan, B. Mei, R. Qi, T. He, Z. Wang, W. Fang, S. Zaman, Y. Su, S. Ding and B. Y. Xia, Local Spin-State Tuning of Cobalt–Iron Selenide Nanoframes for the Boosted Oxygen Evolution, *Energy Environ. Sci.*, 2021, **14**(1), 365–373, DOI: 10.1039/D0EE03500A.
71 Q. Huang and H. Sheng, Magnetic-Field-Induced Spin Regulation in Electrocatalytic Reactions, *Chem. – Eur. J.*, 2024, **30**(28), e202400352, DOI: 10.1002/chem.202400352.
72 G. Zhou, P. Wang, H. Li, B. Hu, Y. Sun, R. Huang and L. Liu, Spin-State Reconfiguration Induced by Alternating Magnetic Field for Efficient Oxygen Evolution Reaction, *Nat. Commun.*, 2021, **12**(1), 4827, DOI: 10.1038/s41467-021-25095-4.
73 K. S. Exner and H. Over, Beyond the Rate-Determining Step in the Oxygen Evolution Reaction over a Single-Crystalline IrO2(110) Model Electrode: Kinetic Scaling Relations, *ACS Catal.*, 2019, **9**(8), 6755–6765, DOI: 10.1021/acscatal.9b01564.
74 Z. He, X. Liu, M. Zhang, L. Guo, M. Ajmal, L. Pan, C. Shi, X. Zhang, Z.-F. Huang and J.-J. Zou, Coupling Ferromagnetic Ordering Electron Transfer Channels and Surface Reconstructed Active Species for Spintronic Electrocatalysis of Water Oxidation, *J. Energy Chem.*, 2023, **85**, 570–580, DOI: 10.1016/j.jechem.2023.06.043.
75 T. Wang, H. He, Z. Meng, S. Li, M. Xu, X. Liu, Y. Zhang, M. Liu and M. Feng, Magnetic Field-Enhanced Electrocatalytic Oxygen Evolution on a Mixed-Valent Cobalt-Modulated LaCoO3

Catalyst, *ChemPhysChem*, 2023, **24**(6), e202200845, DOI: 10.1002/cphc.202200845.
76 S. Jiang, F. Chen, L. Zhu, Z. Yang, Y. Lin, Q. Xu and Y. Wang, Insight into the Catalytic Activity of Amorphous Multimetallic Catalysts under a Magnetic Field toward the Oxygen Evolution Reaction, *ACS Appl. Mater. Interfaces*, 2022, **14**(8), 10227–10236, DOI: 10.1021/acsami.1c19936.
77 H. Wang, Y. Dong, J. Ying, Y. Feng, Z.-H. Zhu, Y.-X. Xiao, G. Tian, L. Shen, W. Geng, Y. Lu, S.-M. Wu and X.-Y. Yang, Low-Temperature Magnetic Field-Assisted Synthesis of Highly Crystalline Fe(OH)x and Its Directed Carrier Transfer Effect under Optical-Magnetic Fields, *ACS Catal.*, 2024, **14**(23), 17664–17674, DOI: 10.1021/acscatal.4c04283.
78 S. Ma, K. Wang, M. Rafique, J. Han, Q. Fu, S. Jiang, X. Wang, T. Yao, P. Xu and B. Song, Reconstruction of Ferromagnetic/Paramagnetic Cobalt-Based Electrocatalysts under Gradient Magnetic Fields for Enhanced Oxygen Evolution, *Angew. Chem.*, 2024, **136**(46), e202412821, DOI: 10.1002/ange.202412821.
79 Y. Chen, X. Hu, M. Hong, Y. Zhu, Y. Su, Y. Fan, Z. Cheng, J. Bell, B. Yu and Y. I. Chen, Magnetic Field-Driven Catalysis: Revealing Enhanced Oxygen Reactions in Li-O2 Batteries Using Tailored Magnetic Nanocatalysts, *Adv. Sci.*, 2025, **12**(34), e05633, DOI: 10.1002/advs.202505633.
80 K. Huang, Y. Yan, Y. Yu, T. Yang, L. Qiao, J. Tu, J. Sui, W. Cai, S. Liu and X. Zheng, N, Fe Co-Incorporated CoO Nanoarray Enhanced by Magnetic Field for Efficient Water Oxidation, *EES Catal.*, 2025, **3**(5), 1044–1054, DOI: 10.1039/D5EY00040H.
81 P. Vensaus, Y. Liang, J.-P. Ansermet, J. Fransson and M. Lingenfelder, Spin-Polarized Electron Transport Promotes the Oxygen Reduction Reaction, *ACS Nano*, 2025, **19**(44), 38709–38715, DOI: 10.1021/acsnano.5c14333.
82 Y. Zhu, X. Wang, C. Wang, C. Cai, Z. Zhu, L. Cui, H. Miao, F. Wang, X. Zhu, C. Zhang, T. Zhang and J. Yuan, Insight into Ni-Based Catalytic Interfaces Empowered by the Magnetic-Induced Heating Effect toward Boosting the Oxygen Evolution Reaction, *ACS Appl. Mater. Interfaces*, 2025, **17**(25), 36686–36697, DOI: 10.1021/acsami.5c05457.
83 E. H. Hechter, A. B. Haruna, X.-Y. Yang, M. W. Terban, H. D. Abruña, D. H. Barrett and K. I. Ozoemena, Magnetic Enhancement of High-Entropy Oxide Electrocatalysts for High Areal-Energy Rechargeable Zinc Air Batteries, *Energy Adv.*, 2025, **4**(10), 1229–1240, DOI: 10.1039/D5YA00091B.
84 Z. Zhang, J. Li, J. Qian, Z. Li, L. Jia, D. Gao and D. Xue, Significant Change of Metal Cations in Geometric Sites by Magnetic-Field Annealing FeCo2O4 for Enhanced Oxygen Catalytic Activity, *Small*, 2022, **18**(7), 2104248, DOI: 10.1002/smll.202104248.
85 Z. Zhang, L. Jia, T. Li, J. Qian, X. Liang, D. Xue and D. Gao, In-Situ Magnetic Field Enhanced Performances in Ferromagnetic FeCo2O4 Nanofibers-Based Rechargeable Zinc–Air Batteries, *J. Energy Chem.*, 2023, **78**, 447–453, DOI: 10.1016/j.jechem.2022.12.038.
86 L. Zhang, J. Peng, Y. Yuan and K. Peng, Magnetic Enhancement of Oxygen Evolution Reaction Performance of NiCo-Spinel Oxides, *Nanotechnology*, 2021, **32**(50), 505716, DOI: 10.1088/1361-6528/ac28d6.
87 W. Kiciński, J. P. Sęk, E. Matysiak-Brynda, K. Miecznikowski, M. Donten, B. Budner and A. M. Nowicka, Enhancement of PGM-Free Oxygen Reduction Electrocatalyst Performance for Conventional and Enzymatic Fuel Cells: The Influence of an External Magnetic Field, *Appl. Catal., B*, 2019, **258**, 117955, DOI: 10.1016/j.apcatb.2019.117955.
88 H. Li, Q. Quan, H. Dong, Y. Zhang, P. Xie, D. Chen, D. Yin, C.-Y. Wong and J. C. Ho, Hierarchical Spin-Polarized Nanosheet Array for Boosting Ampere-Level Water Oxidation Under Magnetic Field, *Adv. Funct. Mater.*, 2025, **35**(20), 2420810, DOI: 10.1002/adfm.202420810.
89 X. Ren, T. Wu, Y. Sun, Y. Li, G. Xian, X. Liu, C. Shen, J. Gracia, H.-J. Gao, H. Yang and Z. J. Xu, Spin-Polarized Oxygen Evolution Reaction under Magnetic Field, *Nat. Commun.*, 2021, **12**(1), 2608, DOI: 10.1038/s41467-021-22865-y.
90 A. A. Yaroslavtsev, A. P. Menushenkov and R. V. Chernikov, Resonant inelastic X-ray scattering (RIXS) on magnetic $EuCo_2P_2$-based systems, *Jetp Lett*, 2012, **96**, 44–48, DOI: 10.1134/S0021364012130152.
91 D. Takegami, T. Aoyama, T. Okauchi, T. Yamaguchi, S. Tippireddy, S. Agrestini, M. García-Fernández, T. Mizokawa, K. Ohgushi, K.-J. Zhou, J. Chaloupka, J. Kuneš, A. Hariki and H. Suzuki, Circular Dichroism in Resonant Inelastic X-Ray Scattering: Probing Altermagnetic Domains in MnTe, *Phys. Rev. Lett.*, 2025, **135**(19), 196502, DOI: 10.1103/512v-n5f9.
92 S. Ajmal, J. Huang, A. Kumar, J. Guo, M. Tabish, M. A. Mushtaq, M. M. Alam and G. Yasin, Magnetically Tuned Spintronic Interfaces in Electrocatalysis: Advanced Mechanistic Understanding, Reactivity Kinetics and Challenges, *Nano Energy*, 2025, **141**, 111134, DOI: 10.1016/j.nanoen.2025.111134.
93 L. Pasteur Researches on the Molecular Dissymmetry of Natural Organic Products: Presented to the Chemical Society of Paris, January 20 and February 3, Translated from ''Leçons de Chimie Professées En 1860.'' 1860.
94 J. Gal, Louis Pasteur, Language, and Molecular Chirality. I. Background and Dissymmetry, *Chirality*, 2010, **23**(1), 1–16, DOI: 10.1002/chir.20866.
95 G. Vantomme and J. Crassous, Pasteur and Chirality: A Story of How Serendipity Favors the Prepared Minds, *Chirality*, 2021, **33**(10), 597–601, DOI: 10.1002/chir.23349.
96 J. Gal, Molecular Chirality in Chemistry and Biology: Historical Milestones, *Helv. Chim. Acta*, 2013, **96**(9), 1617–1657, DOI: 10.1002/hlca.201300300.
97 H. D. Flack, Louis Pasteur's Discovery of Molecular Chirality and Spontaneous Resolution in 1848, Together with a Complete Review of His Crystallographic and Chemical Work, *Acta Crystallogr., Sect. A: Found. Crystallogr.*, 2009, **65**(5), 371–389, DOI: 10.1107/S0108767309024088.
98 K. Mislow, In Molecular Chirality, *Topics in Stereochemistry*, ed E. S. Denmark, 1999, Vol. 22, pp. 1–82, DOI: 10.1002/9780470147313.ch1.
99 P. Cintas, 150 Years of the Tetrahedral Carbon: A Toast to Chirality, *Chirality*, 2025, **37**(2), e70022–e70022, DOI: 10.1002/chir.70022.
100 J. R. Brandt, F. Salerno and M. J. Fuchter, The Added Value of Small-Molecule Chirality in Technological Applications, *Nat. Rev. Chem.*, 2017, **1**(6), 0045, DOI: 10.1038/s41570-017-0045.
101 G. H. Fecher, J. Kübler and C. Felser, Chirality in the Solid State: Chiral Crystal Structures in Chiral and Achiral Space Groups, *Materials*, 2022, **15**(17), 5812, DOI: 10.3390/ma15175812.
102 W. H. Brooks, W. C. Guida and K. G. Daniel, The Significance of Chirality in Drug Design and Development, *Curr. Top. Med. Chem.*, 2011, **11**(7), 760–770, DOI: 10.2174/156802611795165098.
103 L. D. Barron, *Molecular Light Scattering and Optical Activity*, Cambridge University Press, 2004, DOI: 10.1017/CBO9780511535468.
104 R. Naaman and D. H. Waldeck, Spintronics and Chirality: Spin Selectivity in Electron Transport Through Chiral Molecules, *Annu. Rev. Phys. Chem.*, 2015, **66**, 263–281, DOI: 10.1146/annurev-physchem-040214-121554.
105 R. Naaman and D. H. Waldeck, Chiral-Induced Spin Selectivity Effect, *J. Phys. Chem. Lett.*, 2012, **3**(16), 2178–2187, DOI: 10.1021/jz300793y.
106 B. P. Bloom, Y. Paltiel, R. Naaman and D. H. Waldeck, Chiral Induced Spin Selectivity, *Chem. Rev.*, 2024, **124**(4), 1950–1991, DOI: 10.1021/acs.chemrev.3c00661.
107 M. Büttiker, Absence of Backscattering in the Quantum Hall Effect in Multiprobe Conductors, *Phys. Rev. B: Condens. Matter Mater. Phys.*, 1988, **38**(14), 9375–9389, DOI: 10.1103/PhysRevB.38.9375.
108 A. Gupta, A. Kumar, D. K. Bhowmick, C. Fontanesi, Y. Paltiel, J. Fransson and R. Naaman, Does Coherence Affect the Multielectron Oxygen Reduction Reaction?, *J. Phys. Chem. Lett.*, 2023, **14**(42), 9377–9384, DOI: 10.1021/acs.jpclett.3c02594.
109 Y. Liang, K. Banjac, K. Martin, N. Zigon, S. Lee, N. Vanthuyne, F. A. Garcés-Pineda, J. R. Galán-Mascarós, X. Hu, N. Avarvari and M. Lingenfelder, Enhancement of Electrocatalytic Oxygen Evolution by Chiral Molecular Functionalization of Hybrid 2D Electrodes, *Nat. Commun.*, 2022, **13**(1), 3356, DOI: 10.1038/s41467-022-31096-8.
110 Y. Zong, C. Zhang and H. Cao, Chiral Functionalization of Solid Surfaces with Amino Acid Derivatives: Diazonium Grafting Regulated by Enantioselective Processes, *Dalton Trans.*, 2022, **51**(39), 14906–14911, DOI: 10.1039/D2DT02418G.

111 J. Ran, M. Si and D. Gao, Co@CoO Chiral Nanostructures Enabling Efficient Oxygen Electrocatalysis by Modulated Spin-Polarization, *Chem. Eng. J.*, 2024, **493**, 152545, DOI: 10.1016/j.cej.2024.152545.
112 A. Balo, M. Yasmin, U. Utkarsh, U. K. Gosh, R. Choudhury and K. Banerjee Ghosh, Tuning the Spin Polarization of Covalently Coupled CoFe2O4–Reduced Graphene Oxide through a Chiral Metal Support for Electrochemical Oxygen Reduction, *ACS Appl. Energy Mater.*, 2025, **8**(8), 5144–5152, DOI: 10.1021/acsaem.5c00095.
113 J. Guo, A. Hsu, D. Chu and R. Chen, Improving Oxygen Reduction Reaction Activities on Carbon-Supported Ag Nanoparticles in Alkaline Solutions, *J. Phys. Chem. C*, 2010, **114**(10), 4324–4330, DOI: 10.1021/jp910790u.
114 R. Zhou and S. Z. Qiao, Silver/Nitrogen-Doped Graphene Interaction and Its Effect on Electrocatalytic Oxygen Reduction, *Chem. Mater.*, 2014, **26**(20), 5868–5873, DOI: 10.1021/cm502260m.
115 Y. Sang, F. Tassinari, K. Santra, W. Zhang, C. Fontanesi, B. P. Bloom, D. H. Waldeck, J. Fransson and R. Naaman, Chirality Enhances Oxygen Reduction, *Proc. Natl. Acad. Sci. U. S. A.*, 2022, **119**(30), e2202650119, DOI: 10.1073/pnas.2202650119.
116 A. Vadakkayil, C. Clever, K. N. Kunzler, S. Tan, B. P. Bloom and D. H. Waldeck, Chiral Electrocatalysts Eclipse Water Splitting Metrics through Spin Control, *Nat. Commun.*, 2023, **14**(1), 1067, DOI: 10.1038/s41467-023-36703-w.
117 M. Ai, L. Pan, C. Shi, Z.-F. Huang, X. Zhang, W. Mi and J.-J. Zou, Spin Selection in Atomic-Level Chiral Metal Oxide for Photocatalysis, *Nat. Commun.*, 2023, **14**(1), 4562, DOI: 10.1038/s41467-023-40367-x.
118 D. Mandler, Chiral Self-Assembled Monolayers in Electrochemistry, *Curr. Opin. Electrochem.*, 2018, **7**, 42–47, DOI: 10.1016/j.coelec.2017.09.030.
119 J. Yu, Y. Wang, L. Zhu, H. Jiang, J. Hao, Y. Zhang, M. Liu, J. Li, X. Ji and W. Li, Chirality Induces the Self-Assembly To Generate a 3D Porous Spiral-like Polyhedron as Metal-Free Electrocatalysts for the Oxygen Reduction Reaction, *ACS Appl. Mater. Interfaces*, 2019, **11**(49), 45596–45605, DOI: 10.1021/acsami.9b14775.
120 Y. S. Park, J. Lee, H. Lee, J. B. Park, J. Yun, C. U. Lee, S. Moon, S. Lee, S. Kim, J. H. Kim, D. Kim, J. Han, D.-W. Kim and J. Moon, Elucidating the Chirality-Induced Spin Selectivity Effect of Co-Doped NiO Deposited on Ni Foam for Highly Stable Zn–Air Batteries, *ACS Appl. Mater. Interfaces*, 2025, **17**(12), 18228–18242, DOI: 10.1021/acsami.4c20630.
121 L. Gaolatlhe, R. Barik, S. C. Ray and K. I. Ozoemena, Voltammetric Responses of Porous Co3O4 Spinels Supported on MOF-Derived Carbons: Effects of Porous Volume on Dopamine Diffusion Processes, *J. Electroanal. Chem.*, 2020, **872**, 113863, DOI: 10.1016/j.jelechem.2020.113863.
122 Y. Chen, J. Wang, Z. Yu, Y. Hou, R. Jiang, M. Wang, J. Huang, J. Chen, Y. Zhang and H. Zhu, Functional Group Scission-Induced Lattice Strain in Chiral Macromolecular Metal-Organic Framework Arrays for Electrocatalytic Overall Water Splitting, *Appl. Catal., B*, 2022, **307**, 121151, DOI: 10.1016/j.apcatb.2022.121151.
123 Y. Li, L. Qiu, R. Tian, Z. Liu, L. Yao, L. Huang, W. Li, Y. Wang, T. Wang and B. Zhou, Chirality Engineering of Nanostructured Copper Oxide for Enhancing Oxygen Evolution from Water Electrolysis, *Small*, 2024, **20**(52), 2408248, DOI: 10.1002/smll.202408248.
124 D. Barik, U. Utkarsh and K. Banerjee Ghosh, Spin-Controlled Electrocatalysis: An out-of-the-Box Strategy for the Advancement of Electrochemical Water Splitting, *Chem. Commun.*, 2025, **61**(34), 6226–6245, DOI: 10.1039/D5CC01305D.
125 J. Zhu, X. Peng, P. Xi, C. Jia and D. Gao, Dual-Channel Regulation of Spin Polarization Achieves 1 + 1 > 2 Electrocatalytic Performance in Spinel Ferrites, *Nano Lett.*, 2025, **25**(26), 10337–10344, DOI: 10.1021/acs.nanolett.5c01462.
126 X. Tao, L. Hou, X. Wang, J. Jin, H. Li and F. Gao, Iron and Oxygen Vacancies Co-Modulated Adsorption Evolution and Lattice Oxygen Dual-Path Mechanism for Water Oxidation, *Nat. Commun.*, 2025, **16**(1), 8788, DOI: 10.1038/s41467-025-63844-x.
127 R. Tian, L. Huang, Y. Li, D. Zhang, S. Ju, B. Zhou and L. Yao, Spin-Blockade Effect of Chiral Multi-Branch Au Nanoparticles for Mediating Oxygen Evolution Reaction of Electro-Catalytic Water Splitting, *Chem. Eng. J.*, 2025, **520**, 165517, DOI: 10.1016/j.cej.2025.165517.
128 Y. Liang, S. O. Parreiras, S. Lee, K. Banjac, V. Boureau, J. M. Gallego, X. Hu, D. Écija and M. Lingenfelder, *Operando* Nanoscale Characterization Reveals Fe Doping of Ni Oxide Enhances Oxygen Evolution Reaction via Fragmentation and Formation of Dual Active Sites, *Angew. Chem.*, 2025, **137**(10), DOI: 10.1002/ange.202419521.
129 X. Wang, M. Peralta, X. Li, P. V. Möllers, D. Zhou, P. Merz, U. Burkhardt, H. Borrmann, I. Robredo, C. Shekhar, H. Zacharias, X. Feng and C. Felser, Direct Control of Electron Spin at an Intrinsically Chiral Surface for Highly Efficient Oxygen Reduction Reaction, *Proc. Natl. Acad. Sci. U. S. A.*, 2025, **122**(9), DOI: 10.1073/pnas.2413609122.
130 Z. Bian, Y. Nakano, K. Miyata, I. Oya, M. Nobuoka, Y. Tsutsui, S. Seki and M. Suda, Chiral van Der Waals Superlattices for Enhanced Spin-Selective Transport and Spin-Dependent Electrocatalytic Performance, *Adv. Mater.*, 2023, **35**(48), 2306061, DOI: 10.1002/adma.202306061.
131 T. Zhao, D. Meng, Z. Hu, W. Sun, Y. Ji, J. Han, X. Jin, X. Wu and P. Duan, Enhanced Chiroptic Properties of Nanocomposites of Achiral Plasmonic Nanoparticles Decorated with Chiral Dye-Loaded Micelles, *Nat. Commun.*, 2023, **14**(1), 81, DOI: 10.1038/s41467-022-35699-z.
132 X. Niu, Y. Wang, J. Zhang, X. Yang, H. Li and K. Wang, Tuning Enantioselective Recognition and Synergistic Catalytic Activity by the Heterojunction of a Chiral Polysaccharide Hydrogel Interface Electric Field, *ACS Nano*, 2025, **19**(28), 26019–26030, DOI: 10.1021/acsnano.5c06687.
133 P. J. Jessy, R. R. Deshmukh, R. Patel and N. Patel, Exploring Various Nanomaterials in Enhancing the Performance of Chiral Nematic Liquid Crystal for Blue Phase Display, *J. Mol. Liq.*, 2025, **421**, 126859, DOI: 10.1016/j.molliq.2025.126859.
134 L. Ding, B. Liu, A. Peil, S. Fan, J. Chao and N. Liu, DNA-Directed Assembly of Photonic Nanomaterials for Diagnostic and Therapeutic Applications, *Adv. Mater.*, 2025, **37**(49), 2500086, DOI: 10.1002/adma.202500086.
135 D. B. Tripathy, Inorganic Chiral Nanomaterials: Unveiling Potentials, *Proc. Inst. Mech. Eng., Part N*, 2025, 23977914251353291, DOI: 10.1177/23977914251353291.
136 E. Hemmati, S. Soleimani-Amiri and M. Kurdtabar, A CMC-g-Poly(AA-Co-AMPS)/Fe3O4 Hydrogel Nanocomposite as a Novel Biopolymer-Based Catalyst in the Synthesis of 1,4-Dihydropyridines, *RSC Adv.*, 2023, **13**(24), 16567–16583, DOI: 10.1039/D3RA01389H.
137 Z. Xu, X. Tan, C. Chen, X. Wang, R. Sui, Z. Zhuang, C. Zhang and C. Chen, Recent Advances in Microenvironment Regulation for Electrocatalysis, *Natl. Sci. Rev.*, 2024, 11, DOI: 10.1093/nsr/nwae315.
138 J. Luo, Y. Cheng, Z.-W. Gong, K. Wu, Y. Zhou, H.-X. Chen, M. Gauthier, Y.-Z. Cheng, J. Liang and T. Zou, Self-Assembled Peptide Functionalized Gold Nanopolyhedrons with Excellent Chiral Optical Properties, *Langmuir*, 2020, **36**(2), 600–608, DOI: 10.1021/acs.langmuir.9b03366.
139 J. Guo, Y. Duan, Y. Liu, H. Li, Y. Zhang, C. Long, Z. Wang, Y. Yang and S. Zhao, The Biomimetic Engineering of Metal–Organic Frameworks with Single-Chiral-Site Precision for Asymmetric Hydrogenation, *J. Mater. Chem. A*, 2022, **10**(12), 6463–6469, DOI: 10.1039/D1TA08319H.
140 S. Maniappan, C. Dutta, D. M. Solís, J. M. Taboada and J. Kumar, Surfactant Directed Synthesis of Intrinsically Chiral Plasmonic Nanostructures and Precise Tuning of Their Optical Activity through Controlled Self-Assembly, *Angew. Chem., Int. Ed.*, 2023, **62**(21), e202300461, DOI: 10.1002/anie.202300461.
141 K. Chae, N. A. R. Che Mohamad, J. Kim, D.-I. Won, Z. Lin, J. Kim and D. Ha Kim, The Promise of Chiral Electrocatalysis for Efficient and Sustainable Energy Conversion and Storage: A Comprehensive Review of the CISS Effect and Future Directions, *Chem. Soc. Rev.*, 2024, **53**(18), 9029–9058, DOI: 10.1039/D3CS00316G.
142 H. C. Honig, S. Mostoni, Y. Presman, R. Z. Snitkoff-Sol, P. Valagussa, M. D'Arienzo, R. Scotti, C. Santoro, M. Muhyuddin and L. Elbaz, Morphological and Structural Design through Hard-Templating of PGM-Free Electrocatalysts for AEMFC Applications, *Nanoscale*, 2024, **16**(23), 11174–11186, DOI: 10.1039/D4NR01779J.
143 Y. Gorlin, B. Lassalle-Kaiser, J. D. Benck, S. Gul, S. M. Webb, V. K. Yachandra, J. Yano and T. F. Jaramillo, In Situ X-Ray Absorption Spectroscopy Investigation of a Bifunctional Manganese Oxide Catalyst with High Activity for Electrochemical Water

Oxidation and Oxygen Reduction, *J. Am. Chem. Soc.*, 2013, **135**(23), 8525–8534, DOI: 10.1021/ja3104632.
144 X. Yu, Y. Cheng, Y. Li, F. Polo-Garzon, J. Liu, E. Mamontov, M. Li, D. Lennon, S. F. Parker, A. J. Ramirez-Cuesta and Z. Wu, Neutron Scattering Studies of Heterogeneous Catalysis, *Chem. Rev.*, 2023, **123**(13), 8638–8700, DOI: 10.1021/acs.chemrev.3c00101.
145 D. H. Barrett and A. Haruna, Artificial Intelligence and Machine Learning for Targeted Energy Storage Solutions, *Curr. Opin. Electrochem.*, 2020, **21**, 160–166, DOI: 10.1016/j.coelec.2020.02.002.
146 J. R. Rouxel and S. Mukamel, Molecular Chirality and Its Monitoring by Ultrafast X-Ray Pulses, *Chem. Rev.*, 2022, **122**(22), 16802–16838, DOI: 10.1021/acs.chemrev.2c00115.
147 T. Georgiou, J. L. Palma, V. Mujica, S. Varela, M. Galante, V. J. Santamaría-García, L. Mboning, R. N. Schwartz, G. Cuniberti and L.-S. Bouchard, Enantiospecificity in NMR Enabled by Chirality-Induced Spin Selectivity, *Nat. Commun.*, 2024, **15**(1), DOI: 10.1038/s41467-024-49966-8.
148 C. Santana Santos, B. N. Jaato, I. Sanjuán, W. Schuhmann and C. Andronescu, *Operando* Scanning Electrochemical Probe Microscopy during Electrocatalysis, *Chem. Rev.*, 2023, **123**(8), 4972–5019, DOI: 10.1021/acs.chemrev.2c00766.
149 X. Xu, W. Liu, Y. Huang, W. Li and S. Che, Magnetic Shielding Mechanism and Structure Design of Composites at Low Frequency: A Review, *J. Magn. Magn. Mater.*, 2023, **570**, 170509, DOI: 10.1016/j.jmmm.2023.170509.
150 R. Mach-Batlle, M. G. Bason, N. Del-Valle and J. Prat-Camps, Tailoring Magnetic Fields in Inaccessible Regions, *Phys. Rev. Lett.*, 2020, **125**(17), 177204, DOI: 10.1103/PhysRevLett.125.177204.